USE OF COCONUT FIBERS IN HIGH STRENGTH CONCRETE FOR IMPROVING DUCTILITY

MS STRUCTURES DISSERTATION

BY

WAQAS AHMAD
MS-Structures 2015
00000117610

MS THESIS ADVISOR

Dr. Syed Hassan Farooq

NUST Institute of Civil Engineering (NICE)
School of Civil & Environmental Engineering (SCEE)
National University of Sciences and Technology (NUST), Islamabad, Pakistan

February, 2018

This is to certify that

Thesis titled

"USE OF COCONUT FIBERS IN HIGH STRENGTH CONCRETE FOR IMPROVING DUCTILITY"

Submitted by

Waqas Ahmad

Fall 2015-MS Structural Engineering

00000117610

Has been accepted towards the partial fulfilment

of

the requirements for the award of degree of

Master of Science in Structural Engineering

____

Dr. Syed Hassan Farooq (Supervisor)

NUST Institute of Civil Engineering (NICE)
National University of Sciences and Technology (NUST),
Islamabad, Pakistan

THESIS ACCEPTANCE CERTIFICATE

Certified that final copy of MS thesis written by Mr. Waqas Ahmad, Registration No. 00000117610, of MS Structural Engineering 2015 Batch (NICE), has been vetted by undersigned, found completed in all respects as per NUST Statutes/Regulations, is free of plagiarism, errors, and mistakes and is accepted as partial fulfillment for award of MS degree. It is further certified that necessary amendments as pointed out by GEC members of the scholar have been incorporated in the said thesis.

Signature: ____________________________

Name of Supervisor: Dr. Syed Hassan Farooq

Date: ________________________________

Signature: ____________________________

Head of Department: Dr. Rao Arsalan Khushnood

Date: ________________________________

Signature: ____________________________

Dean: Dr. Syed Muhammad Jamil

Date: ________________________________

DEDICATION

I dedicate this research to my family especially my beloved father.

ACKNOWLEDGEMENTS

All praise to ALLAH who gave me power to complete my research thesis. I would like to express my sincere gratitude to my advisor Dr. Syed Hassan Farooq and GEC members Dr. Rao Arslan Khushnood and Dr. Muhammad Usman for their continuous support, encouragement and guidance throughout my research. I am deeply indebted to Engr. Mehran Khan who provided me helpful materials and constantly guided me during my thesis.

I am really indebted to my brother Engr. Ayaz Ahmad and friends Engr. Asmatullah, Engr. Abid-Ur-Rehman and Engr. Abdur Rasheed who helped me during experimental work.

I am also thankful to Sika Pakistan (Pvt.) Ltd for providing silica fume and super-plasticizer used in this research.

TABLE OF CONTENTS

LIST OF TABLES

LIST OF FIGURES

LIST OF ABBREVIATIONS

CEC	cracked energy absorbed in compression
CEF	cracked energy absorbed in flexure
CES	cracked energy absorbed in splitting
CF	coconut fibers
CFRC	coconut fiber reinforced concrete
CFR-HSC	coconut fiber reinforced high strength concrete
E_{static}	static modulus of elasticity
FM	fineness modulus
FRC	fiber reinforced concrete
FRHSC	fiber reinforced high strength concrete
HPC	high performance concrete
HSC	high strength concrete
MOR	modulus of rupture
NSC	normal strength concrete
OPC	ordinary Portland cement
PC	plain concrete
PCEC	post-crack energy absorbed in compression
PEC	pre-crack energy absorbed in compression
PEF	pre-crack energy absorbed in flexure

PES	pre-crack energy absorbed in splitting
SEM	scanning electron microscopy
SF	silica fume
STS	splitting-tensile strength
TEC	total energy absorbed in compression
TEF	total energy absorbed in flexure
TES	total energy absorbed in splitting
TIC	toughness index in compression
TIF	toughness index in flexure
TIS	toughness index in splitting
W/C	water cement ratio
ε_u	ultimate strain
ε_y	yield strain
μ	strain ductility
σ	compressive strength

ABSTRACT

Now a days concrete with enhanced properties such as high strength, toughness and durability is an essential demand of construction industry. High strength concrete (HSC) have enhanced mechanical properties than normal strength concrete (NSC). HSC has a variety of applications in construction industry such as high rise buildings, long span bridges and hydraulic structures. The factor which limits the utilization of HSC is its brittleness which is more than NSC. Therefore, controlling the brittleness of HSC is an important aspect in civil engineering construction industry which needs to be investigated. The mechanical properties of HSC can be improved by addition of fibers. As compared to artificial fibers, natural fibers are cheap and locally available. Among the natural fibers, coconut fibers have the highest toughness. In this study, mechanical properties of coconut fiber reinforced high strength concrete (CFR-HSC) are investigated. The effectiveness of coconut fibers (CF) in HSC is determined by comparing the mechanical properties of CFR-HSC with that of HSC having the same mix design. The properties of HSC are taken as a reference. The influence of 25 mm, 50 mm and 75 mm long fibers and 0.5%, 1%, 1.5% and 2% contents, by mass of cement are investigated. The microstructure of CFR-HSC is studied using scanning electron microscopy (SEM). The experimental results reveal that CFR-HSC show improved compressive, splitting-tensile and flexural strengths, strain ductility, energies absorbed and toughness indices than that of HSC. As compared to HSC, CFR-HSC showed enhanced post-cracking behavior which results in controlling the brittleness and ultimately improved the ductility. The overall best results are obtained for CFR-HSC having 50 mm long fibers and 1.5% fiber content. Thus, CFR-HSC with optimized length and content can be used for civil engineering structures.

Keywords: High strength concrete; coconut fiber; mechanical properties; strain ductility; microstructure.

CHAPTER 1

INTRODUCTION

1.1. BACKGROUND

Concrete is a widely used construction material because of its advantages such as economical, locally available and widely applicable (Afroughsabet and Ozbakkaloglu 2015). Now a days concrete having higher strength, durability, toughness and ductility is an essential demand of construction industry (Breitenbuecher 1999). High strength concrete (HSC) have improved mechanical properties than normal strength concrete (NSC). However, HSC has a brittle behavior than that of NSC (Afroughsabet and Ozbakkaloglu 2015). In civil engineering construction industry, HSC has a variety of applications such as high rise/tall buildings, hydraulic structures and long span bridges. In high rise buildings, HSC decreases the dead load of structure and also avoids larger sized columns (Swamy 1985). Also in long span bridges, HSC reduces the dead load of girders by reducing their section sizes and thus reduces the size of piers (Rabbat and Russel 1982). HSC is more durable than NSC as it possesses high density and low permeability which increases its resistance against deleterious effects (Mbessa and Pera 2001 and Chan et al. 2000).

1.2. PROBLEM STATEMENT

With the development of construction industry in modern civil engineering there is an essential demand for new types of concretes having improved properties such as high strength, durability, toughness and ductility (Farnam et al. 2010). Examples of new type of concrete are high strength concrete (HSC), high performance concrete (HPC) and fiber reinforced high strength concrete (FRHSC). Such concretes shows substantial improved properties over conventional concrete (Lim and Ozbakkaloglu 2014). The factor which limits the utilization of HSC is its brittleness which is more than NSC. Additionally for the production of high strength concrete supplementary cementitious materials like silica fume, fly ash and blast-furnace slag are used as part of binder (Yazici 2007). Use of these cementitious materials as replacement of cement reduces the porosity of concrete in long term (Rashiddadash et al. 2014). On the other hand, with the addition of these cementitious materials the brittleness of concrete is also increased (Nili and Afroughsabet 2010). Therefore, controlling the brittleness by improving the ductility of high strength concrete (HSC) is an important aspect in concrete technology which needs to be investigated.

1.3. RESEARCH OBJECTIVES

i. To study the mechanical properties of coconut fiber reinforced high strength concrete (CFR-HSC).

ii. To improve ductility of high strength concrete (HSC) by addition of coconut fibers in different proportions.

1.4. RESEARCH METHODOLOGY

i. The mechanical properties of high strength concrete (HSC) are compared with that of coconut fiber reinforced high strength concrete (CFR-HSC).

ii. Coconut fiber of lengths 25 mm, 50 mm and 75 mm and contents 0.5%, 1%, 1.5% and 2%, by mass of cement, are incorporated in HSC to study its various mechanical properties.

iii. Mix design ratio for cement, sand and aggregate and water cement (W/C) ratio are kept same for both HSC and CFR-HSC.

iv. Cylinders are casted for compressive and splitting-tensile strength tests while beams are casted for flexural strength tests.

v. The compressive strength (σ), static modulus of elasticity (E_{static}), energy absorbed in compression, toughness index in compression (TIC), strain ductility (μ), splitting tensile strength (STS), energy absorbed in splitting, toughness index in splitting (TIS), modulus of rupture (MOR), energy absorbed in flexure and toughness index in flexure (TIF) are studied.

vi. The optimized length and content of coconut fibers is determined from the obtained results.

1.5. THESIS OVERVIEW

Chapter 1 contains background, problem statement, research objectives, methodology and thesis layout.

Chapter 2 includes literature review. It comprises of previous studies on high strength concrete (HSC), fiber reinforced concrete (FRC), and coconut fiber reinforced composites. It also includes applications of HSC and FRC.

Chapter 3 explain research methodology. It covers material used, mix design, casting procedure, specimens detail and testing setups.

Chapter 4 includes results obtained from tests performed and analysis of obtained results. It also covers the comparison of various properties of HSC and CFR-HSC with increasing fiber length and content.

Chapter 5 contains discussions over obtained results, optimization of coconut fibers in HSC and comparison of compressive, splitting-tensile and flexural properties of HSC and CFR-HSC.

Chapter 6 includes conclusions and recommendations.

CHAPTER 2

LITERATURE REVIEW

2.1. GENERAL

The mechanical properties of concrete can be enhanced by using natural or artificial fibers (Khan and Ali 2016). Eswari el al. (2008) reported that concrete strength, ductility, damage tolerance in flexure and energy absorption capacity can be enhanced by incorporation of fibers in concrete. The addition of fibers in concrete delays the crack propagation and improves stress distribution in the matrix at the time of loading (Brandt 2008). Now a days natural fibers are incorporated in concrete to produce a material with improved strength, toughness, ductility and durability properties (Kuder and Shah 2010 and Ezeldin and Balaguru 1989). Natural fibers have been used by researchers as an alternative of synthetic fibers in composites like concrete (Aggarwal 1992, Al-Oraimi and Seibi 1995 and Ali et al. 2013). Natural fibers are very cheap as compared to synthetic fibers and are locally available in many countries. Natural fibers includes coconut, bamboo, jute, palm, sisal, hemp, banana, kenaf bast, pineapple leaf, flax, ramine bast, sugarcane, abaca leaf and cotton fibers. Use of these fibers as a construction material can improve the properties of composite at relatively low cost. As compared to synthetic fibers like steel they are flexible and easy to handle, especially when they are used in higher quantities (Ali et al. 2012). Among the natural fibers coconut fibers have the highest toughness and are capable of taking 4-6 times more strain than that of other fibers (Ali et al. 2012 and Munawar et al. 2007).

2.2. HIGH STRENGTH CONCRETE (HSC)

According to ACI concrete having compressive strength over 41 MPa (6000 psi) is called HSC (ACI 363R-92). HSC possesses other improved properties in addition to higher strength as compared to that of NSC. Production of HSC requires quality materials (fine and coarse aggregates), higher binder quantity, smaller water-binder ratio and supplementary cementitious materials (silica fume, fly ash, blast furnace slag etc.). Super-plasticizer may be used for the reduction of water-binder ratio.

There are many advantages of HSC over NSC. Due to higher compressive strength, HSC used in compression members like columns and piles will results in reduced member sizes. Reduction in column sizes of building increases the available floor space. Also because of higher compressive strength per unit volume per unit weight will results in reduced overall dead load of structure on foundation. However, HSC possess more brittle behavior as compared to that of NSC (Afroughsabet and Ozbakkaloglu 2015).

2.2.1. Effect of silica fume on HSC

ACI committee 234 reported the significance of silica fume as replacement of cement in concrete. It was reported that silica fume improves the microstructure of concrete and hence resulting in more durable concrete. Also silica fume improves the bond between paste and aggregate (i.e. ITZ) which results in enhanced mechanical properties.

Mazloom et al. (2004) investigated the effect of silica fume on mechanical properties of HSC. Silica fume was added in HSC with the cement replacement of 6%, 10% and 15%. The results were compared with that of ordinary Portland cement (OPC) concrete. It was observed that with the addition of silica fume 28 days compressive strength of concrete increased from 17.2% to 20.7% and modulus of elasticity increased from 3.2% to 10.8%. The maximum compressive strength and modulus of elasticity were obtained at 15% silica fume content.

Johari et al. (2011) studied the influence of silica fume of engineering properties of HSC. Silica fume was added 5%, 10% and 15% as replacement of cement. Experimental study reveals that silica fume has a significant effect on compressive strength (σ) of HSC. The σ at 28 days increased with increasing silica fume content. With the addition of silica fume σ increased from 21.9% to 35.5% as compared to that of HSC without silica fume. The influence of silica fume on static modulus of elasticity (E_{static}) was observed a very small. The E_{static} increased from 3.4% to 8.2% with the addition of silica fume. The optimum results were obtained with the addition of 15% silica fume as replacement of cement. It was also reported that addition of silica fume result in the reduction of porosity of concrete.

Hassan et al. (2000) investigated the effect of silica fume on the properties of HSC. Silica fume was added in concrete having mix design ratio of 1:2:3 (cement:sand:aggragate). Silica fume replaced 10% by weight of OPC. It was reported that silica fume increased compressive strength by 10%. Also the addition of silica fume results in denser concrete and reduced the porosity by 25%, as compared to that of OPC concrete. Also in comparison to OPC concrete silica fume reduced the permeability of concrete up to 87%.

2.2.2. Applications of HSC

HSC is generally used in the members of structures such as columns and beams of buildings as it decreases the sizes of members and increases the available floor space. Recently, concrete with compressive strengths approaching 138 MPa (20,000 psi) have been used in cast-in-place buildings (Peterman and Carrasquillo 1986). HSC is also used for the construction of highway bridges. HSC used in reinforced or pre-stressed concrete girders results in greater span lengths than NSC girders. Also, because of greater capacities of individual girder may enable a decrease in the number of girders required. Thus, HSC also has an economical advantage over NSC. The main applications for HSC are in high rise/tall buildings, hydraulic structures, long span bridges and pre-stressed concrete structures (French et. al 1998).

2.3. FIBER REINFORCED CONCRETE (FRC)

Concrete containing discrete fibers added at the time of mixing is called fiber reinforced concrete (FRC). Concrete tensile strength is very less as compared to its compressive strength and has a brittle behavior. Incorporation of fibers improves the mechanical properties of concrete (Ali et al. 2012 and Khan and Ali 2016). FRC possess enhanced properties high strength, durability, energy absorption capacity and damage tolerance in flexure (Eswari et al.) The main role of fibers in concrete is bridging action which controls crack propagation and leading to enhanced post-cracking behavior.

Khan and Ali (2018) used hair and wave polypropylene fibers in concrete to study its influence on concrete roads (rigid pavements). Hair and wave polypropylene fibers of 5 cm and content 0.8%, by total concrete volume was incorporated in concrete. Mix design ratio was 1:3.33:1.67:0.71 (cement:sand:aggregate:water) for controlled mix (CM) as well as for FRCs. Properties of hair fiber reinforced concrete (HFRC) and wave polypropylene fiber reinforced concrete (WPFRC) were compared with that of CM. It was found that density of HFRC and WPFRC reduced by 8.9% and 4.9%, respectively, as compared to that of CM. The reduction in density is due to addition of less density hair and wave polypropylene fibers and creation of voids. It was concluded from the experimental work that compressive, flexural and splitting-tensile strengths of HFRC are improved by 12.4%, 16.2% and 19.1%, respectively, and that of WPFRC are improved by 11.7%, 21.5% and 17.5%, respectively, as compared to that of CM. It was reported that using HFRC and WPFRC in concrete roads may result in better performance and can reduce cost per lane per km by 3% and 1.7% by use of HFRC and WPFRC, respectively.

Zia and Ali (2017) studied the effect of jute fiber reinforced concrete (JFRC), nylon fiber reinforced concrete (NFRC) and polypropylene fiber reinforced concrete (PPFRC) for controlling the rate of cracking in canal lining. Concrete having mix proportion of 1:3:1.5:0.7 (cement: sand: aggregate: water) was used for plain concrete (PC) as well as for FRCs. Jute, nylon and polypropylene fibers of 50 mm length and 5% content, by mass of cement were used. Compressive strength of JFRC and NFRC were reduced by 36% and 31%, respectively, while that of PPFRC increased by 1% as compared to that of plain concrete (PC). Splitting-tensile strength of JFRC and NFRC were reduced by 21% and 11%, respectively, while that of PPFRC increased by 5% than that of PC. Modulus of rupture (MOR) of JFRC, NFRC and PPFRC were increased by 8%, 10%

and 34%, respectively, as compared to that of PC. It was concluded that PPFRC showed the better performance as compared to others. It was reported that PPFRC may result in controlling rate of cracking in canal-lining.

Khan and Ali (2016) investigated the mechanical properties of glass fiber reinforced concrete (GFRC) and nylon fiber reinforced concrete (NFRC) for controlling early age micro-cracking in bridge decks. Glass and nylon fibers of 50 mm length and 5% content, by mass of cement were incorporated in concrete with the mix design ratio for cement, sand and aggregate of 1:3.33:1.67 and water cement (W/C) ratio of 0.71. The properties of GFRC and NFRC were compared with that of PC. It was observed that density of GFRC and NFRC were reduced by 2.4% and 1.8%, respectively, as compared to that of PC because of addition of low density fibers. From the experimental work it was observed that compressive strength of GFRC and NFRC were reduced by 2.8% and 5.8%, respectively, than that of PC. The reason for reduced compressive strength is reported as dilution of cement (fibers addition in same mix design). However, it was observed that GFRC and NFRC showed much better compressive post-cracking behavior than that of PC. There is an increase of 11% and 8.4% in splitting-tensile strength of GFRC and NFRC, respectively, and also 5.6% and 3% in flexural strength of GFRC and NFRC, respectively, as compared to that of PC. It was concluded that GFRC and NFRC may result in controlling early age micro-cracking in bridge decks.

Song and Hwang (2004) studied the mechanical properties of high strength steel fiber reinforced concrete (HSFRC). Steel fibers were incorporated in HSC with the volume fractions of 0.5%, 1%, 1.5% and 2%. The maximum compressive strength was achieved at 1.5% volume fraction which was 15.3% higher than that of HSC. The splitting-tensile strength and modulus of rupture maximum at 2% volume fraction which were 98.3% and 126.6%, respectively, higher than that of HSC.

Afroughsabet and Ozbakkaloglu (2015) investigated the mechanical and durability properties of HSC containing polypropylene and steel fibers. Polypropylene fibers of 12 mm length and volume fractions of 0.15%, 0.30% and 0.45% were used. Steel fibers (hooked-end) of 60 mm length and volume fractions of 0.25%, 0.5%, 0.75% and 1% were incorporated in HSC. From the tests performed higher compressive strengths were observed for all fiber reinforced specimens. The reasons reported for the increase in compressive strength are the ability of fibers to restrain the crack extension, changes the direction of cracks and delays crack propagation. With the addition of polypropylene fibers the compressive strength of increased from 5% to 15% and with the addition of steel fibers compressive strength increased from 7% to 18% as compared to that of HSC. The maximum compressive strength was obtained at 1% volume fraction of steel fibers. The addition of fibers showed significant improvement in splitting-tensile strength (STS). It was observed that with increasing fiber volume fraction results in increased STS. STS increased from 11% to 20% with the addition of polypropylene fibers and from 13% to 58% with the addition of steel fibers. Similarly trend was observed for flexural strength of HSC due to fiber addition. With the addition of polypropylene fibers flexural strength increased from 5% to 12% and with the addition of steel fibers flexural strength increased from 9% to 61%. The maximum flexural strength was obtained with addition of steel fibers having 1% volume fraction.

Eren and Celik (1997) studied the effect of steel fibers and silica fume on properties of HSC. Hooked-end steel fibers of 30 mm, 50 mm and 60 mm length and volume fractions of 0.5%, 1% and 2% were added in HSC. Silica fume was also added in two different fractions i.e. 5% and 10% by weight of cement. The splitting-tensile strength was maximum at 10% silica fume and 2% fiber content which was 129.9% higher than PC. The maximum compressive strength was obtained at 10% silica fume and 1% fiber content which was 28.27% increased as compared to that of PC.

2.3.1. Applications of FRC

The main areas of FRC applications are:

- Runway, aircraft parking and pavement
- Tunnel lining and slope stabilization
- Blast/impact resistant structures
- Thin shell, walls, pipes and manholes
- Shotcrete
- Precast elements
- Composite decks
- Roof tiles

2.4. COCONUT FIBERS

The outer shell of coconut contains coconut fibers. Coconut fibers are also called coir, cocos nucifera and arecaceae (Palm). There are two types of coconut fibers;

(i) Brown fibers

(ii) White fibers

Brown fibers are extracted from matured coconuts and are thick, strong and have high abrasion resistance. Whereas white fibers are extracted from immature coconuts and are smoother, finer and also weaker. In civil engineering, only brown fibers are used. (Ali et al. 2012).

According to the official website of International Year for Natural Fibers 2009, worldwide mainly in Sri Lanka and India, approximately 500,000 tons of coconut fibers are produced. The estimated total value of coconut fiber is $100 million. The main exporters are Sri Lanka and India followed by Indonesia, Vietnam, Thailand and Philippines. Approximately half of the coconut fibers are exported in the form of raw fiber.

The main advantages of coconut fibers include resistant to fungi and rot, moth-proof, excellent resistant against temperature, unaffected by dampness and moisture, resilient, tough, flexible and durable. Among the natural fibers coconut fibers have the maximum toughness and are capable of taking 4-6 times more strain than that of other fibers (Munawar et al. 2007).

2.5. COCONUT FIBER REINFORCED COMPOSITES

Researchers have used coconut fibers in normal strength concrete (NSC) and mortar to study its various mechanical properties. Some researcher’s contributions are as follows;

Ali et al. (2012) investigated the mechanical properties of coconut fiber reinforced concrete (CFRC) using different lengths and content of coconut fibers. In normal strength concrete (NSC) having cement, sand and aggregate ratio of 1:2:2 and water cement ratio (W/C) of 0.48, coconut fibers were incorporated having lengths 2.5 cm, 5 cm and 7.5 cm and content 1%, 2%, 3% and 5%, by mass of cement. The incorporation of coconut fibers in concrete showed improved mechanical properties than plain concrete (PC). It was concluded that the best overall results obtained for CFRC with 5 cm long fibers and 5% content, by mass of cement. Increase in compressive strength (σ), modulus of rupture (MOR), total toughness index (TTI) was up to 4%, 21%, 2% and 910%, respectively, and decrease in static modulus of elasticity (E_{static}), splitting tensile strength (STS) and density was up to 6%, 2% and 3%, respectively, as compared to that of plain concrete (PC).

Ali et al. (2013) investigated the bond strength between coconut fiber and concrete. The influence of fiber diameter, length, treatment before use and concrete mix design ratios on the bond strength between coconut fiber and concrete is investigated. It was concluded from the experimental work that maximum fiber bond strength in concrete is achieved when (i) fiber is thick, (ii) embedment length is 30 mm, (iii) treated with boiling water and (iv) concrete mix design ratio is 1:3:3.

Baruah and Talukdar (2007) studied mechanical properties of concrete having fibers with volume fractions ranging from 0.5% to 2% and compared the results with that of PC. Coconut fibers of 4 cm length and 0.4 mm average diameter having volume fractions of 0.5%, 1%, 1.5% and 2% was incorporated in concrete having cement, sand and aggregate ratio of 1:1.67:3.64 and water cement ratio (W/C) of 0.535. The compressive strength (σ), splitting tensile strength (STS), modulus of rupture (MOR) and toughness index for PC and CFRC are shown in Table 2.1. The best overall performance was reported for CFRC having 2% volume fraction.

Table 2.1: Comparison of PC and CFRC mechanical properties according to Baruah and Talukdar (2007)

Fiber volume fraction (%)	Compressive strength (MPa)	Split tensile strength (MPa)	Modulus of rupture (MPa)	Toughness Index (I_5)
-	21.42	2.88	3.25	1.934
0.5	21.70	3.02	3.38	2.165
1.0	22.74	3.18	3.68	2.109
1.5	25.10	3.37	4.07	2.706
2.0	24.35	3.54	4.16	2.345

Ramli et al. (2013) studied the influence of coconut fibers in concrete in aggressive environment (i.e. under water structures). Coconut fibers of diameter 0.32 mm and length 20-30 mm were incorporated in concrete in four different fractions, i.e. 0.6%, 1.2%, 1.8% and 2.4%, by mass of cement. The experimental work reveals that incorporation of fibers in concrete improved compressive and flexural strengths up to 13% and 9%, respectively, as compared to that of PC. It was concluded that incorporation of coconut fibers in concrete not only improved the compressive and flexural strengths but it also results in improved durability than that of PC.

Slate (1976) studied the effect of coconut fibers on compressive and flexural strength of mortar with cement-sand ratio of 1:2.75 and 1:4. Fiber content used was 0.08%, 0.16%

and 0.32% by total mass of mortar. The properties of coconut fiber reinforced mortar are compared with that of plain mortar. Cylinders (50 mm dia. and 100 mm height) and beams (50 mm x 50 mm cross section and 200 mm length) were casted and cured for 8 days before testing. It was found that incorporation of fibers increased both compressive and flexural strengths for both mix design ratios as compared to that of plain mortar. However, with increasing fiber content a decreasing trend in strengths of coconut fiber reinforced mortar was observed.

Aziz et al. (1981) investigated the mechanical properties of cement paste composites with different length and content of coconut fibers. Three different lengths 25 mm, 38 mm and 50 mm and volume fractions of 2%, 3%, 4%, 5% and 6% were incorporated in cement paste composite. The optimum results were obtained with 38 mm fiber length and 4% content.

John et al. studied the durability of coconut fiber reinforced mortar. The samples were taken from walls of a 12 years old house made with mortar having cement-sand ratio of 1:1.5 and water cement (W/C) ratio of 0.504. The mortar was also reinforced with coconut fibers (2% by volume). It was found that fibers was not damaged when removed from old samples which confirmed the durability of coconut fibers in mortar.

Li et al. (2006) studied the influence of 20 mm and 40 mm coconut fibers in cementitious composites. Mortar was prepared with cement, sand, water and super plasticizer ratio of 1:3:0.43:0.01 by weight. It was concluded that the resulting mortar increased the flexural strength, energy absorption and ductility up to 12%, 1680% and 1740%, respectively, than that of plain mortar.

Reis (2006) investigated the flexural strength, fracture toughness and fracture energy of fiber reinforced epoxy polymer concrete by performing third-point loading tests. Coconut, sugarcane bagasse and banana fibers were used as reinforcement. From the experimental investigation it was found that highest fracture toughness and energy was obtained with coconut fiber reinforced polymer concrete. The flexural strength was increased up to 25% with coconut fibers.

CHAPTER 3

METHODOLOGY

3.1. MATERIALS AND THEIR PROPERTIES

3.1.1. Cement

Ordinary Portland cement (OPC) has different ingredient and hence different types. In this experimental program cement with the brand name of Bestway used for casting all specimens.

3.1.2. Sand

In this experimental program Lawrencepur sand was used which was procured from a local supplier. From physical observation and sieve analysis the sand was found of reasonable quality. The fineness modulus (FM) of sand was 2.7 which is in the ASTM range. Sand was washed before use to eliminate the clay particles. The specific gravity and water absorption of sand was 2.66 and 1.36%, respectively.

3.1.3. Coarse aggregate

Coarse aggregate from the quarry of Margala was used in this experimental program. Coarse aggregate with the maximum size of 12.5 mm is used. The specific gravity and water absorption of coarse aggregate was 2.68 and 0.68%, respectively. Coarse aggregate was washed and dried before use.

3.1.4. Coconut fibers

Coconut fibers were imported from Sri-Lanka having length of 200 mm. The fibers were cut in the desired lengths (i.e. 25 mm, 50 mm and 75 mm). Coconut fibers were soaked into water for 30 min to soften the fibers and then washed. Soaking and washing was repeated three times to remove all dust particles. Fibers were then dried in open air before use.

(a) (b) (c)

Figure 3.1: Coconut fibers used in experimental program having lengths (a) 25 mm (b) 50 mm and (c) 75 mm

3.1.5. Silica fume and super-plasticizer

Silica fume and super plasticizer was provided by Sika Pakistan private Ltd. The function of silica fume is to provide strength while that of super-plasticizer is to maintain workability. There is usually a low W/C ratio in high strength concrete. By using the super-plasticizer in such concretes helps in mixing and placing.

3.2. MIX DESIGN AND CASTING PROCEDURE

Table 3.1 shows the mix proportions used for various specimens. For mixing all the ingredients of concrete pan type mixer was used. For preparing high strength concrete (HSC) all the materials (cement, sand, aggregates and silica fume) were put in the mixer pan. Super-plasticizer was mixed in water and added to the mixer pan. The mixer was rotated for 3 minutes. Ali et al. (2012) reported the method for mixing coconut fibers in concrete to achieve uniform dispersion of fibers in the matrix and to avoid balling effect. Silica fume was mixed with cement. For preparing CFR-HSC a layer of coconut fibers was uniformly spread in the mixer pan and this first layer of fibers was hidden by spreading sand, aggregates and cement. Then another layer of fibers was uniformly spread over it followed by layers of sand, aggregate and cement. This process was repeated until all the material was put into the pan mixer. Approximately three quarters of the total water containing super-plasticizer was added in the pan and the mixer was rotated for 2 minutes. Then the remaining water was added in the mix and mixer was again rotated for 3 minutes. Total mixing time for CFR-HSC was 5 minutes.

For casting specimens mix was poured in to the molds in three layers and compaction of each layer was done with 25 blows of temping rod for both HSC and CFR-HSC. Since coconut fibers are flexible, there was no apparent damage to the fibers with temping during casting. This observation is based upon visual inspection of few fibers being removed from concrete after temping of a layer in mold. All the specimens were de-molded after 24 hours and cured for 28 days before testing.

Table 3.1: Mix proportions of concrete mixes

Concrete Type	Mix ID	Cement (kg/m^3)	Sand (kg/m^3)	Coarse Aggregate (kg/m^3)	Water (kg/m^3)	Silica Fume (kg/m^3)	Super-plasticizer (kg/m^3)	Fiber Length (mm)	Fiber Content (%)	Fiber (kg/m^3)
HSC	Mix0	525	785	785	184	52.5	5.25	-	-	-
CFR-HSC	Mix1-0.5	525	785	785	184	52.5	5.25	25	0.5	2.62
	Mix1-1	525	785	785	184	52.5	5.25	25	1	5.25
	Mix1-1.5	525	785	785	184	52.5	5.25	25	1.5	7.88
	Mix1-2	525	785	785	184	52.5	5.25	25	2	10.50
	Mix2-0.5	525	785	785	184	52.5	5.25	50	0.5	2.62
	Mix2-1	525	785	785	184	52.5	5.25	50	1	5.25
	Mix2-1.5	525	785	785	184	52.5	5.25	50	1.5	7.88
	Mix2-2	525	785	785	184	52.5	5.25	50	2	10.50
	Mix3-0.5	525	785	785	184	52.5	5.25	75	0.5	2.62
	Mix3-1	525	785	785	184	52.5	5.25	75	1	5.25
	Mix3-1.5	525	785	785	184	52.5	5.25	75	1.5	7.88
	Mix3-2	525	785	785	184	52.5	5.25	75	2	10.50

3.3. SPECIMENS

Cylinders of 100 mm diameter and 200 mm in height and beams of 100 mm x 100 mm cross section and 500 mm long were prepared for HSC and CFR-HSC. Cylinders were casted for compression and splitting-tensile tests while beams were casted for flexural-strength tests. A set of three specimens for each particular test was prepared. Total of 78 cylinders and 39 beams were casted. Figure 3.2 shows the specimens (cylinders and beams) before and after de-molding.

(a) Casted cylinders in molds

(b) Cylinders after de-molding

(c) Casted beams in molds

(d) Beams after de-molding

Figure 3.2: Specimens in molds and after de-molding

3.4. TESTING PROCEDURE

3.4.1. Slump of fresh concrete

The slump test was performed for all mixes before pouring into molds following ASTM C143/143M-15a for workability determination of HSC. To the best of author’s knowledge, no standard method is available to determine workability of CFR-HSC. Thus the same procedure was used to determine the workability of CFR-HSC. Figure 3.3 shows the slump test performed.

Figure 3.3: Slump test

3.4.2. Density of hardened concrete

The density of HSC in hardened state was measured following ASTM C138/C138M-17a. The same procedure is followed for CFR-HSC for determining its density because of unavailability of respective standards for CFR-HSC.

Figure 3.4: Density measurement

3.4.3. Compressive strength test

ASTM C39/C39M-17b was followed for testing compressive strength of cylinders. All the cylinders were capped with plaster of paris before testing for uniform distribution of load (Figure 3.5). Universal testing machine (UTM) was used for testing all cylinders to study compressive behavior, to calculate compressive strength (σ) and to determine static modulus of elasticity (E_{static}), pre-crack energy absorbed in compression (PEC), cracked energy absorbed in compression (CEC), post-crack energy absorbed in compression (PCEC), total energy absorbed in compression (TEC), toughness index in compression (TIC) and strain ductility (μ) of both HSC and CFR-HSC. The Test was performed in displacement controlled mode with the rate of 1 mm/min during testing. Figure 3.6 shows the experimental setup for compressive strength test.

Figure 3.5: Capping of cylinders

Figure 3.6: Compression testing of cylinder in UTM

3.4.4. Splitting-tensile strength test

ASTM C496/C496M-17 was followed for splitting-tensile strength test of cylinders. Compression testing machine is used for splitting-tensile strength test to study splitting-tensile behavior, to calculate splitting-tensile strength (STS) and to determine pre-crack energy absorbed in splitting (PES), cracked energy absorbed in splitting (CES), total energy absorbed in splitting (TES) and toughness index in splitting (TIS) of both HSC and CFR-HSC. During testing loading rate was 0.025 kN/sec. Figure 3.7 shows the experimental setup for splitting-tensile strength test.

Figure 3.7: Splitting tensile strength test setup

3.4.5. Flexural strength test

ASTM C293/C293M-16 was followed for flexural strength testing of beams in UTM to study flexure behavior, to calculate modulus of rupture (MOR) and to determine pre-crack energy absorbed in flexure (PEF), cracked energy absorbed in flexure (CEF), total energy absorbed in flexure (TEF) and toughness index in flexure (TIF) of both HSC and CFR-HSC. The test was performed in displacement controlled mode with the rate of 0.02 mm/min during testing. Figure 3.8 shows the arrangement for flexural strength test of beams.

Figure 3.8: Arrangement of 3-point load test for beams

3.4.6. Scanning electron microscopy (SEM)

Specimens for SEM analysis measuring 10 mm by 10 mm by 5 mm were prepared from CFR-HSC beams after flexural strength test. Those specimens were washed and dried. Gold-palladium coating was applied on each specimen before SEM analysis. The SEM was performed to study the microstructure of CFR-HSC. In this experiment, interfacial transition zone (ITZ) between aggregate-cement and fiber-cement and pores in the matrix were studied. Figure 3.9 shows the setups for gold-palladium coating and SEM analysis.

(a) Gold-palladium coating (b) SEM equipment

Figure 3.9: SEM analysis setup

CHAPTER 4

TEST RESULTS AND ANALYSIS

4.1. SLUMP OF FRESH CONCRETE

Table 4.1 shows the slump values for all the mixes and percentage decrease in slump of CFR-HSC than that of HSC. The effect on slump with increasing fiber length and content is shown in Figure 4.1. Solid straight line indicates the slump of HSC. All CFR-HSC show decreased slump than HSC. With increasing fiber length from 25 mm to 50 mm slump first increases and then decreases on further increase in fiber length. The possible reasons are:

i. For 25 mm length of fibers, fibers are more in numbers which decreases the workability of concrete.

ii. For 50 mm length of fibers, number of fibers are less as compared to 25 mm fiber length which results in increased slump.

iii. For 75 mm length of fiber, number of fibers are further decreased but longer fibers reduced the workability of concrete.

With increases in fiber content slump decreases. Higher quantity of fibers reduced the workability of fresh concrete. In spite of decreased slump CFR-HSC was found workable.

Table 4.1: Slump of HSC and CFR-HSC

Mix ID	Slump (mm)	% decrease in slump
Mix0	200	
Mix1-0.5	175	12.5
Mix1-1	125	37.5
Mix1-1.5	90	55
Mix1-2	50	75
Mix2-0.5	185	7.5
Mix2-1	160	20
Mix2-1.5	100	50
Mix2-2	75	62.5
Mix3-0.5	160	20
Mix3-1	115	42.5
Mix3-1.5	60	70
Mix3-2	25	87.5

(a)

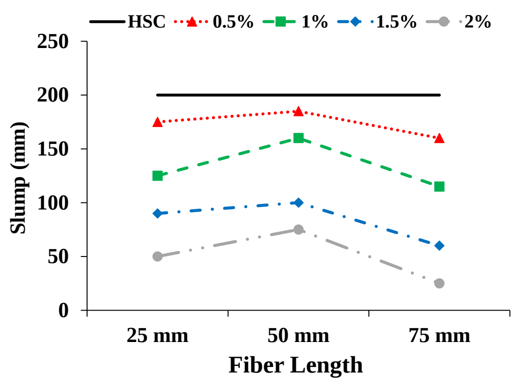

(b)

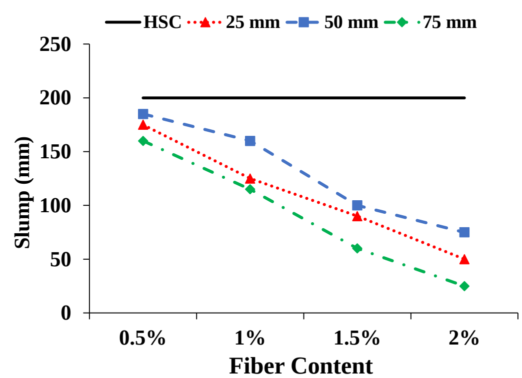

Figure 4.1: Influence on slump (a) fiber length (b) fiber content

4.2. DENSITY OF HARDENED CONCRETE

As expected, CFR-HSC showed decreased density than HSC. The influence on density with increasing fiber length and content is shown in Figure 4.2. With increasing fiber length density of CFR-HSC first increases and then decreases. With the increase in fiber content density decreases. As fibers are light weight itself, their addition in concrete created voids which decreased its density. The density of CFR-HSC with 75 mm fiber length and 2% content reduced by 2.6% than that of HSC. Table 4.2 shows the density of hardened concrete for all mixes and percentage decrease in density of CFR-HSC than that of HSC.

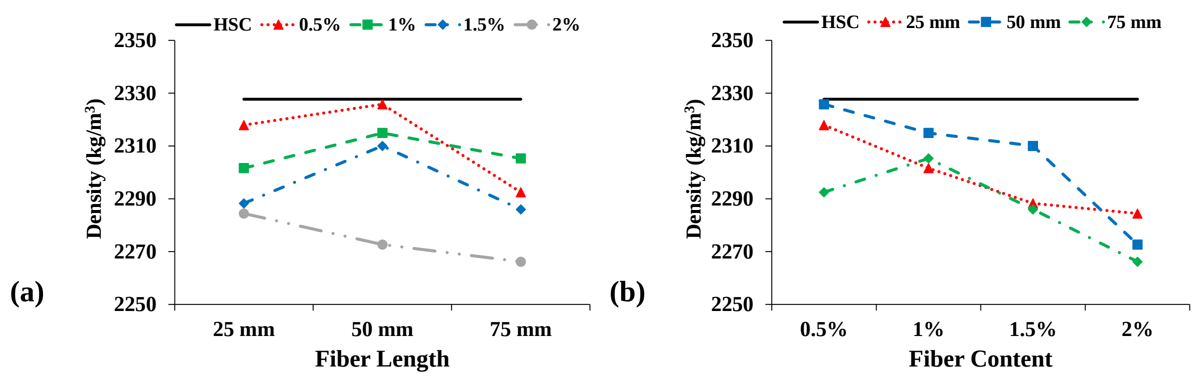

Figure 4.2: Influence on density (a) fiber length (b) fiber content

Table 4.2: Density of HSC and CFR-HSC

Mix ID	Density (kg/m^3)	% decrease in density
Mix0	2327.7	-
Mix1-0.5	2317.9	0.42
Mix1-1	2301.6	1.12
Mix1-1.5	2288.2	1.70
Mix1-2	2284.4	1.86
Mix2-0.5	2325.8	0.08
Mix2-1	2314.9	0.55
Mix2-1.5	2310.0	0.76
Mix2-2	2272.6	2.37
Mix3-0.5	2292.5	1.51
Mix3-1	2305.3	0.96
Mix3-1.5	2286.0	1.79
Mix3-2	2266.1	2.65

4.3. COMPRESSIVE PROPERTIES

4.3.1. Compressive behavior

Combined stress-strain curves for HSC and CFR-HSC with same length and changing content are shown in Figure 4.3. As expected CFR-HSC showed greater strength and strain value than HSC. Also CFR-HSC showed substantial strain energy absorption after the peak stress as compared to that of HSC. At 25 mm fiber length (Figure 4.3a) a little increase in peak stress is observed for all fiber contents while a substantial increase in strain at peak stress is observed at higher fiber contents. At 50 mm fiber length (Figure 4.3b), further increase in peak stress is observed at lower fiber content while maximum strain at peak stress is observed for 1.5% fiber content. For 75 mm fiber length (Figure 4.3c), peak stress and strain at peak stress are reduced as compared to 50 mm fiber length but higher than that of HSC and CFR-HSC with 25 mm fiber length. In Figure 4.4 a comparison is made having same fiber content with changing length. Maximum stress values are obtained at 0.5% fiber content but maximum strain values are obtained at 1.5% fiber content. The optimum result is obtained with 1.5% fiber content and 50 mm length as shown. At 2% fiber content the stress of CFR-HSC is less than that of HSC. This may be due to less workability and non-uniform dispersion of fibers in the mix.

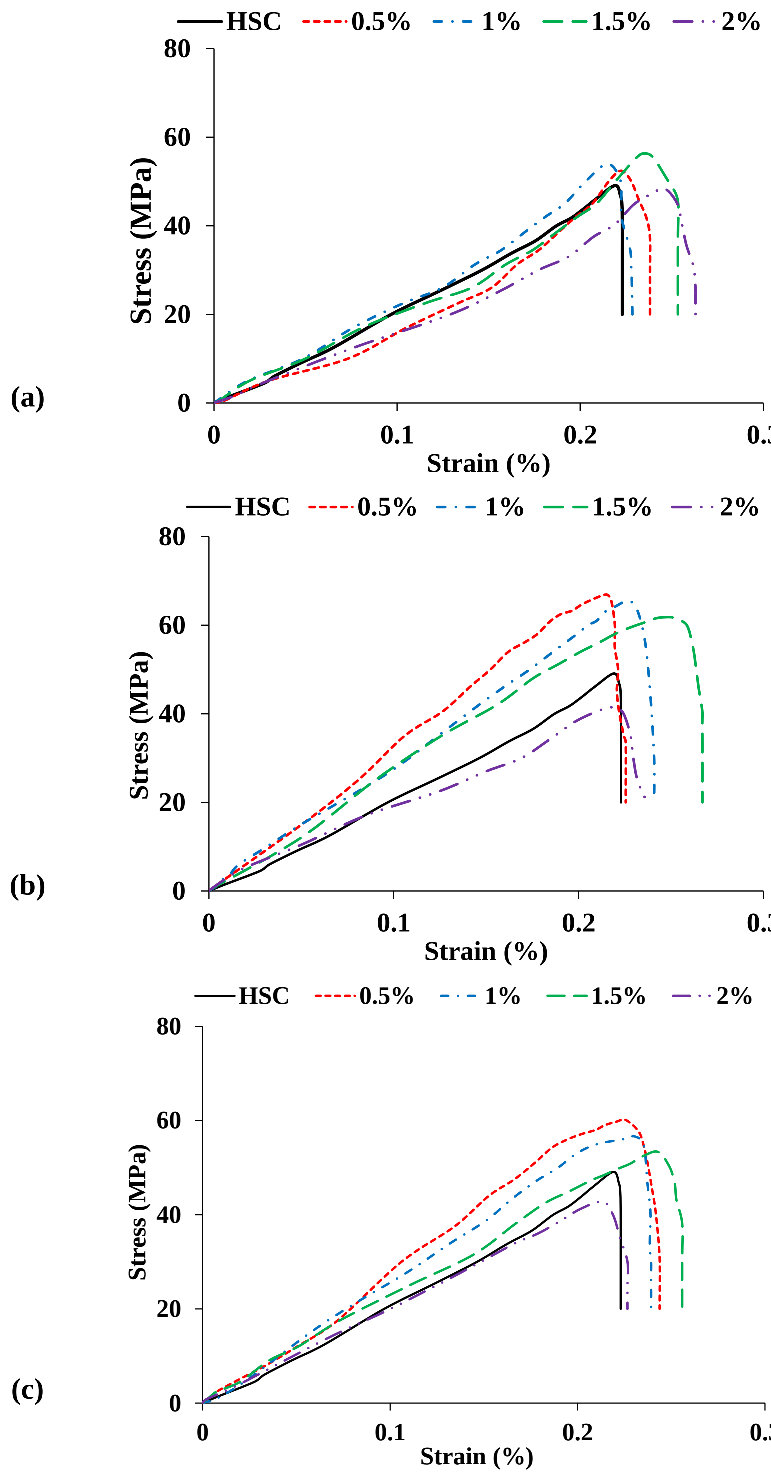

Figure 4.3: Stress-strain curves for HSC and CFR-HSC having (a) 25 mm (b) 50 mm and (c) 75 mm long fibers

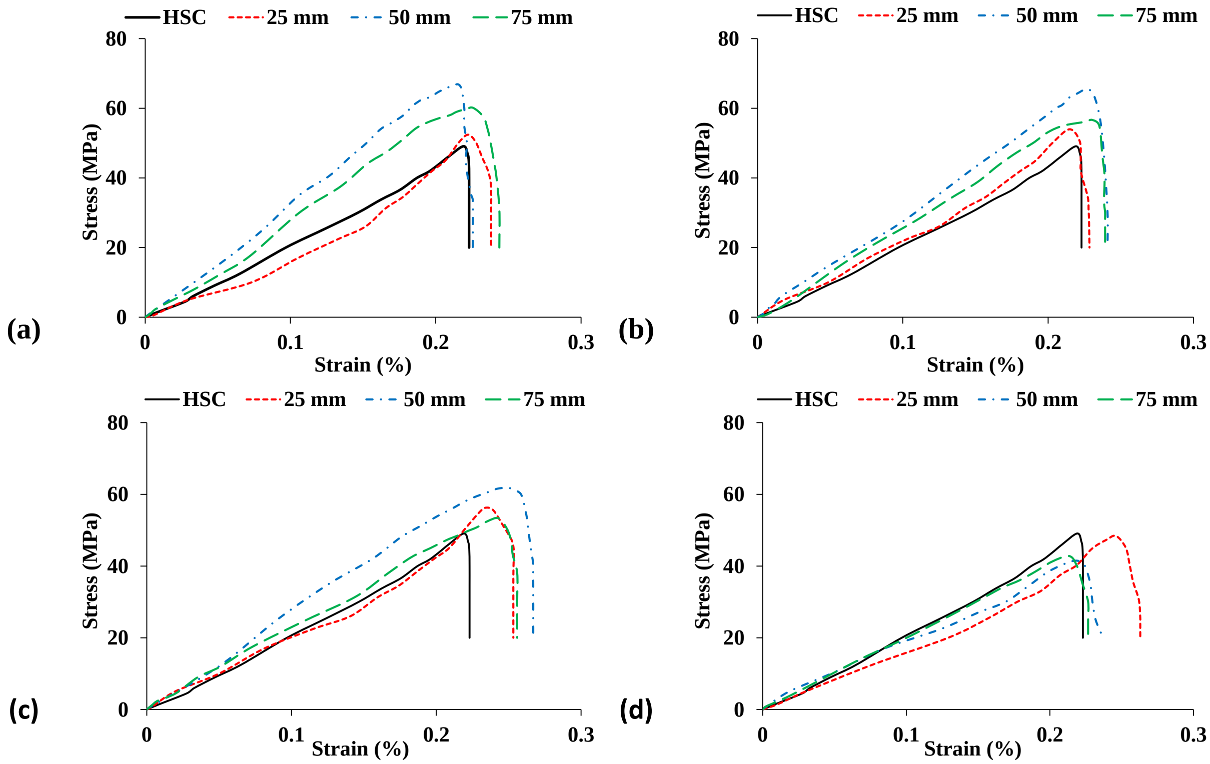

Figure 4.4: Stress-strain curves for HSC and CFR-HSC having (a) 0.5% (b) 1% (c) 1.5% and (d) 2% fiber content

The specimens of HSC and CFR-HSC after compressive strength test are shown in Figure 4.5. At maximum load, concrete pieces from HSC were chipped off while in CFR-HSC pieces of concrete were held together. The reason is the presence of fibers which provided the bridging effect in CFR-HSC. Also it was visually observed that crack width, length and number of cracks were greater in HSC than that of CFR-HSC.

Figure 4.5: HSC and CFR-HSC specimens after compressive strength tests

4.3.2. Static Modulus of Elasticity (E_{static})

Static modulus of elasticity (E_{static}) is calculated as the ratio of stress change to strain change with in the elastic limit. Figure 4.6 shows the effect on E_{static} with increasing fiber length and content. The solid straight line shows the E_{static} of HSC. E_{static} of CFR-HSC decreased with increase in fiber length and content. Only CFR-HSC with 25 mm fiber length and 0.5% and 1% content showed increased E_{static} than that of HSC. All the other CFR-HSC showed decreased E_{static} than that of HSC. E_{static} of CFR-HSC with 50 mm and 75 mm fiber lengths and 2% content reduced by 13.4% than that of HSC.

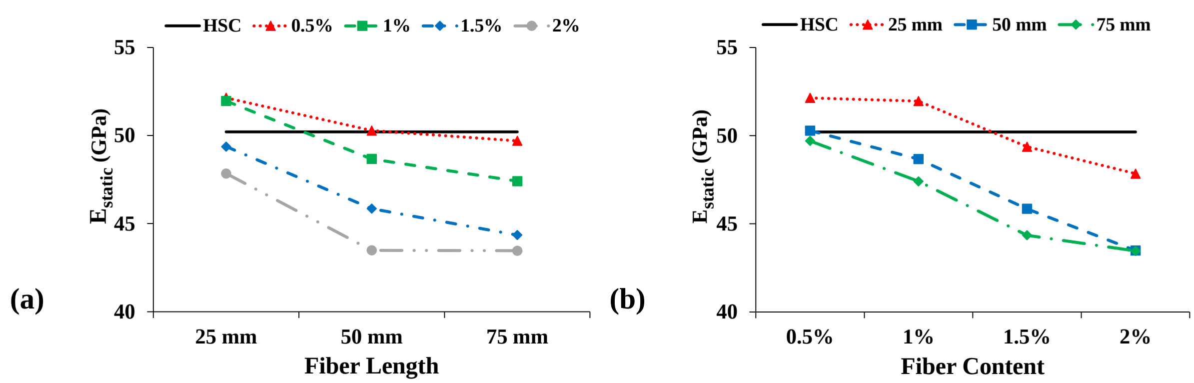

Figure 4.6: Influence on E_{static} (a) fiber length (b) fiber content

4.3.3. Compressive Strength (σ)

Compressive strength (σ) is taken as the maximum stress value from the stress-strain curve. The influence on σ with increasing fiber length and content is shown in Figure 4.7. Solid straight line shows the σ of HSC. The σ of CFR-HSC first increases and then decreases with increasing fiber length. For 25 mm length of fiber σ increased with increasing fiber content up to 1.5% and then decreased when fiber content increased to 2%. However, for 50 mm and 75 mm long fibers σ decreased with the increase in fiber content. The decrease in σ may be due to: (i) the creation of air voids with the addition of fibers in higher content and longer length; (ii) at higher fiber content and length workability of fresh concrete decreased because of which proper compaction was not done during casting specimens; (iii) dilution of cement due to fiber addition.

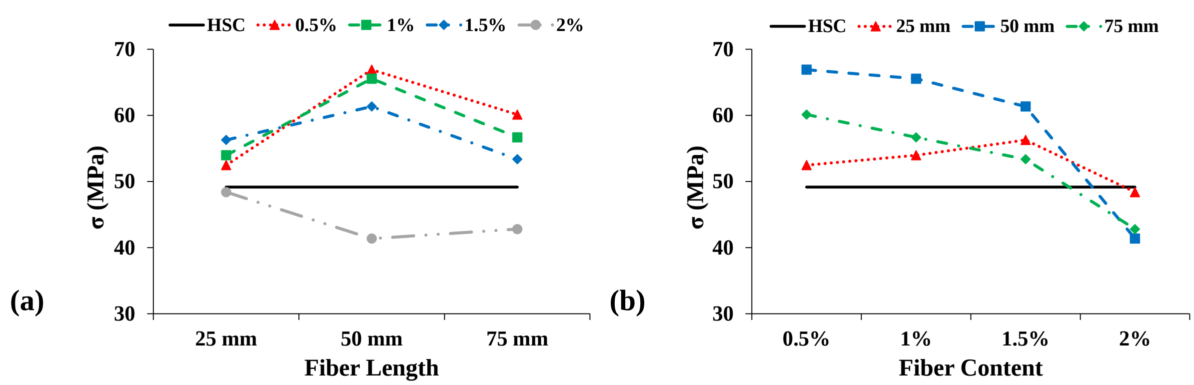

Figure 4.7: Influence on σ (a) fiber length (b) fiber content

4.3.4. Energy absorbed in compression and toughness index

Pre-crack energy absorbed in compression (PEC) is calculated as the area under the stress-strain curve up to the yield stress. Yield stress is taken as the stress at which first visual crack is observed during compressive strength test. The area under the stress-strain curve from yield stress to the peak stress is taken as cracked energy absorbed in compression (CEC). Post-crack energy absorbed in compression (PCEC) is taken as the area under the stress strain curve from peak stress to the ultimate stress. Ultimate stress is taken as the stress after the peak stress drops by 20%. Total energy absorbed in compression (TEC) is calculated as the area under the stress-strain curve from zero to ultimate stress. Toughness index in compression (TIC) is the ratio of total energy absorbed in compression to the pre-crack energy absorbed in compression (i.e. TEC/PEC).

The influence on PEC with increasing fiber length and content is shown in Figure 4.8. Solid straight line shows the PEC of HSC. CFR-HSC show increased PEC as compared to HSC. PEC of CFR-HSC first increases and then decreases with increase in fiber length. With increasing fiber content up to 1.5%, PEC increases and then decreases on further increase in fiber content. PEC of CFR-HSC with 50 mm fiber length and 1.5% content has the maximum value which is 40% higher than that of HSC.

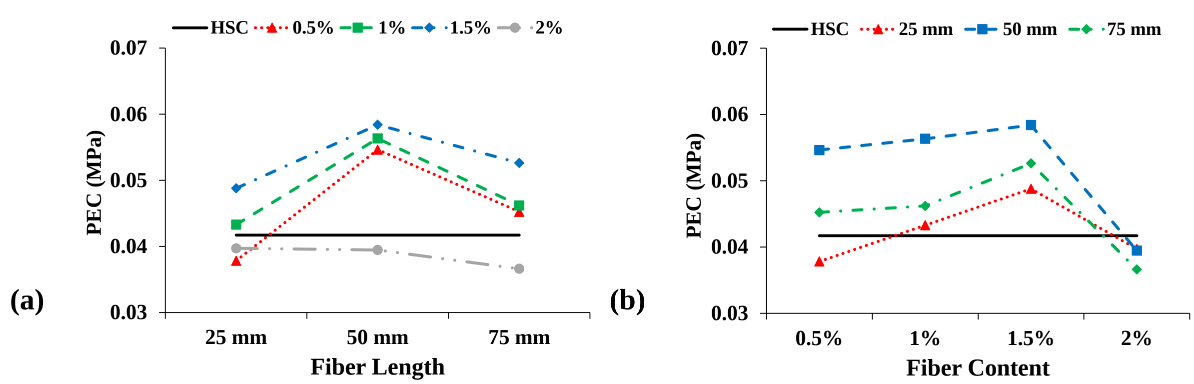

Figure 4.8: Influence on PEC (a) fiber length (b) fiber content

The effect on CEC with increasing fiber length and content is shown in Figure 4.9. As expected, CEC of CFR-HSC is higher than HSC. The addition of fibers provided the significant stress resistance after the first crack by bridging the cracks. CEC of CFR-HSC having 0.5% and 1% fiber content increases with increasing fiber length. Whereas CEC of CFR-HSC having 1.5% and 2% fiber content first increases and then decreases with increasing fiber length. CEC decreases with increase in fiber content. This may be due to creation of air voids in the matrix because of higher fiber content which results in lower energy absorption after the peak stress. CFR-HSC with 50 mm fiber length and 1.5% content has the highest value of CEC which is increased by 98.5% than HSC.

(a)

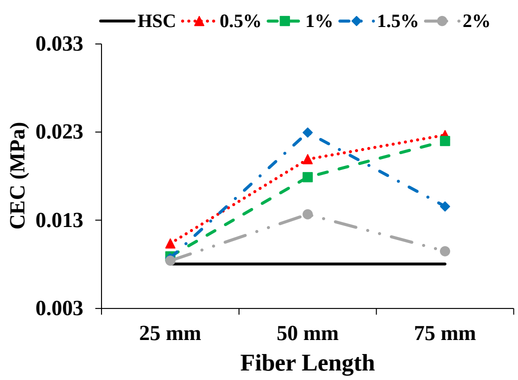

(b)

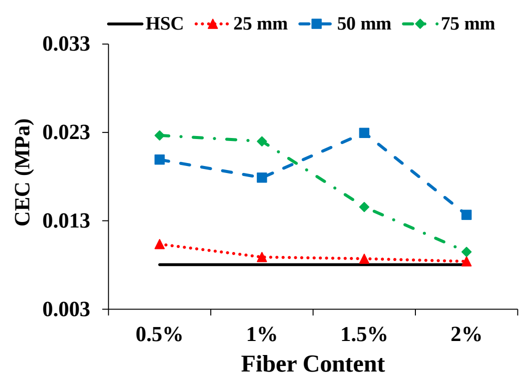

Figure 4.9: Influence on CEC (a) fiber length (b) fiber content

Figure 4.10 shows the influence on PCEC with increasing fiber length and content. The solid straight line is the PCEC of HSC. CFR-HSC shows increased PCEC than HSC because of presence of fibers which provided the capacity to absorb energy after the peak stress by bridging the cracks. PCEC of CFR-HSC having 0.5% fiber content shows approximately same values for all lengths of fiber. For CFR-HSC having 1% and 1.5% fiber content, PCEC first increases and then decreases with increasing fiber length.

However, PCEC of CFR-HSC having 2% fiber content first decreases and then increases with increasing fiber length. With increasing fiber content up to 1.5%, PCEC increases and then decreases on further increase in fiber content. CFR-HSC having 50 mm long fibers shows the maximum values of PCEC. This possible reasons are: (i) at 25 mm fiber length, number of fibers are more for bridging the cracks but their embedment length is short which results in pull-out of fibers; (ii) when fiber length is 50 mm, relatively less number of fibers are there but sufficient embedment length to hold the cracks which results in higher PCEC value; (iii) when fiber length is 75 mm, embedment length is increased but less number of fibers results in fiber breaking and reduced PCEC value.

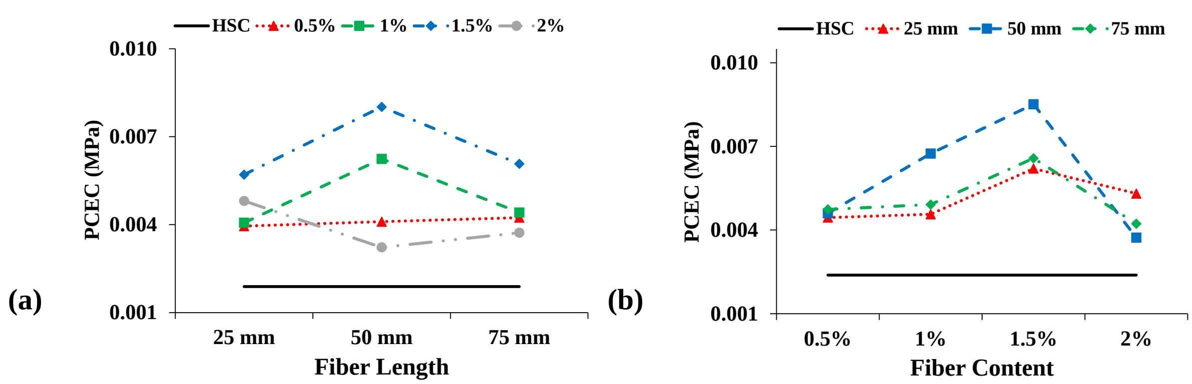

Figure 4.10: Influence on PCEC (a) fiber length (b) fiber content

The influence on TEC with increasing fiber length and content is shown in Figure 4.11. The solid straight line is TEC of HSC. With increasing fiber length TEC of CFR-HSC first increases and then decreases. TEC increases with increasing fiber content up to 1.5% and then decreases on further fiber addition. The possible reasons may be improper compaction and cement dilution at higher fiber content and longer length. The TEC of CFR-HSC with 50 mm fiber length and 1.5% content has increased by 73.2% as compared to that of HSC.

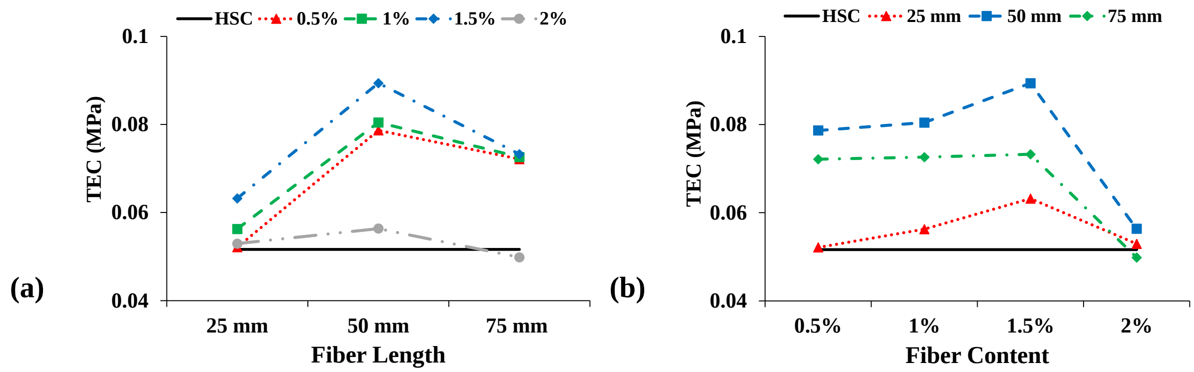

Figure 4.11: Influence on TEC (a) fiber length (b) fiber content

Figure 4.12 shows the effect on TIC with increasing fiber length and content. The solid straight line is that of HSC. TIC of CFR-HSC is always higher than that of HSC as the addition of fibers provide stress resistance especially after the peak stress by bridging the cracks.

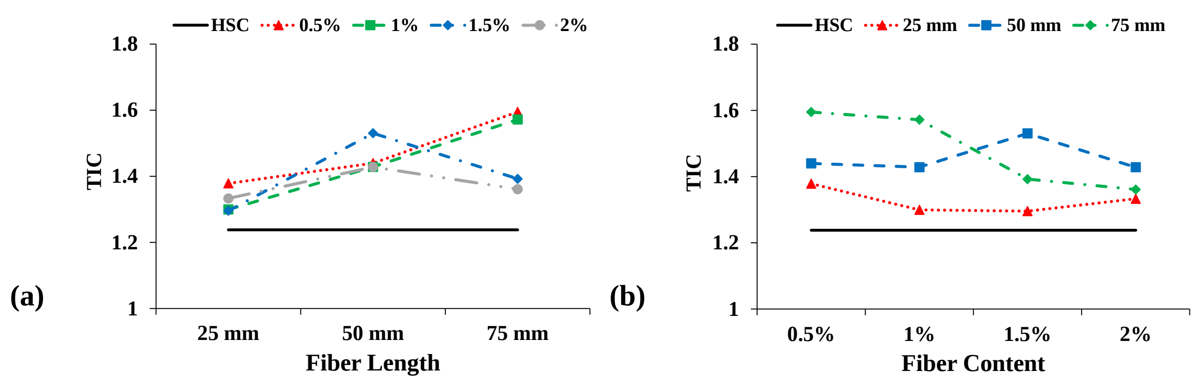

Figure 4.12: Influence on TIC (a) fiber length (b) fiber content

4.3.5. Strain ductility (μ)

Strain ductility (μ) is determined as the ratio of ultimate strain to yield strain (i.e. $\mu = \varepsilon_u/\varepsilon_y$). The effect on μ with increasing fiber length and content is shown in Figure 4.13. The solid straight line is the μ of HSC. CFR-HSC showed increased μ than HSC. Fiber bridging the cracks results in higher strain values after yield stress and hence higher μ is achieved. With increasing fiber length μ first increases and then decreased. With increasing fiber content up to 1.5% μ increases while it decreases upon further increase in fiber content. CFR-HSC having 50 mm long fibers and 1.5% fiber content has the maximum value which is increased by 14.6% than that of HSC. Table 4.3 includes all the compressive properties of HSC and CFR-HSC.

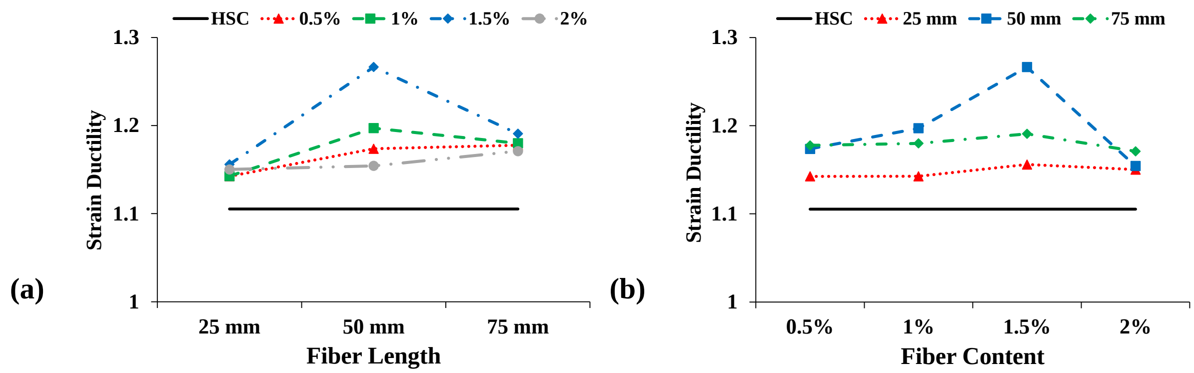

Figure 4.13: Influence on strain ductility (a) fiber length (b) fiber content

Table 4.3: Compressive properties of HSC CFR-HSC

Mix ID	σ (MPa)	MOE (GPa)	PEC (MPa)	CEC (MPa)	PCEC (MPa)	TEC (MPa)	TIC	μ
Mix0	49.14	50.21	0.0417	0.0080	0.0019	0.0516	1.24	1.11
Mix1-0.5	52.47	52.14	0.0378	0.0104	0.0039	0.0521	1.38	1.14
Mix1-1	53.96	51.96	0.0433	0.0089	0.0041	0.0563	1.30	1.14
Mix1-1.5	56.28	49.37	0.0488	0.0087	0.0057	0.0632	1.30	1.16
Mix1-2	48.38	47.84	0.0397	0.0084	0.0048	0.0529	1.33	1.15
Mix2-0.5	66.9	50.28	0.0546	0.0199	0.0041	0.0786	1.44	1.17
Mix2-1	65.54	48.67	0.0563	0.0179	0.0062	0.0804	1.43	1.20
Mix2-1.5	61.34	45.85	0.0584	0.0230	0.0080	0.0894	1.53	1.27
Mix2-2	41.36	43.48	0.0395	0.0137	0.0032	0.0563	1.43	1.15
Mix3-0.5	60.12	49.7	0.0452	0.0227	0.0042	0.0721	1.59	1.18
Mix3-1	56.67	47.41	0.0462	0.0220	0.0044	0.0726	1.57	1.18
Mix3-1.5	53.36	44.35	0.0526	0.0146	0.0061	0.0733	1.39	1.19
Mix3-2	42.79	43.46	0.0366	0.0095	0.0037	0.0498	1.36	1.17

4.4. SPLITTING-TENSILE PROPERTIES

4.4.1. Splitting-tensile behavior

Load-time curve was recorded during the splitting-tensile testing of cylinders. Splitting load-time curve for HSC and CFR-HSC is shown in Figure 4.14. HSC samples were broken into two pieces at peak load while CFR-HSC samples remain in contact at and after the peak load. The test was run up to 10 minutes for all CFR-HSC samples. The presence of fibers in CFR-HSC shows the bridging effect that hold the two pieces of concrete together. The samples of HSC and CFR-HSC after testing are shown in Figure 4.15. The CFR-HSC samples were intentionally separated after testing to observe the fiber failure. Table 4.4 shows the approximate amount of fiber pull-out and broken with increasing fiber length. With increasing fiber length embedment length of fibers in concrete increases which results in decreased amount of fiber pull-out.

Table 4.4: Approximate amount of fiber pull-out and broken with increasing fiber length in STS test

Fiber Length (mm)	Pull out (%)	Broken (%)
25	20	80
50	10	90
75	5	95

(a)

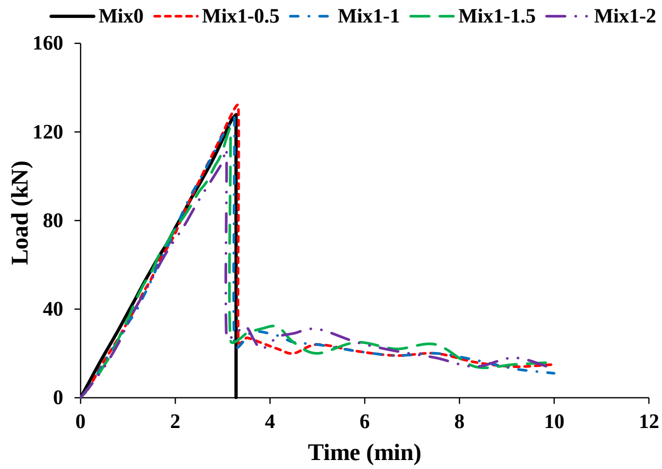

(b)

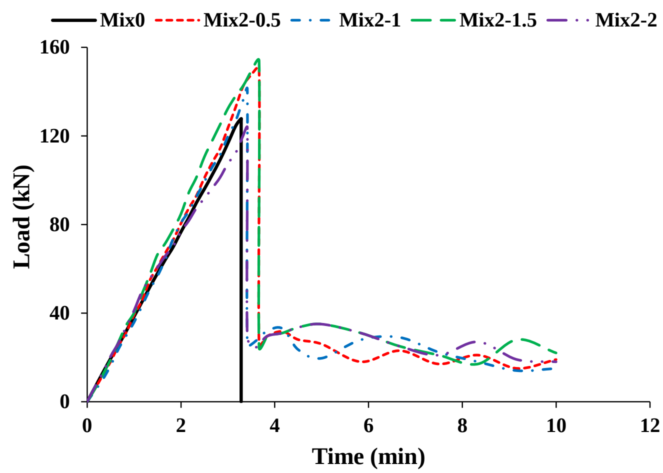

(c)

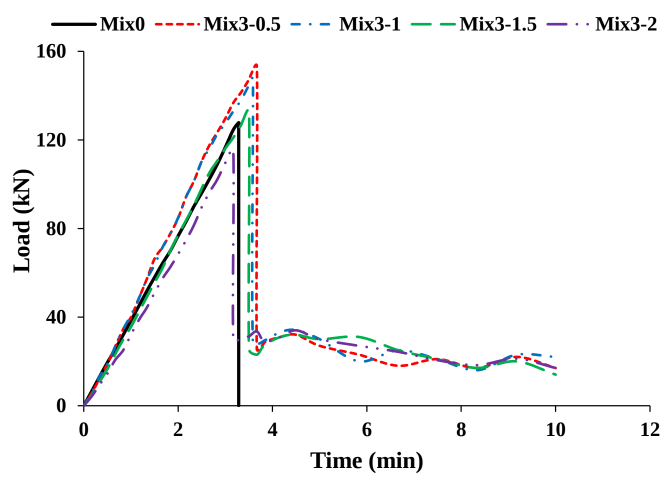

Figure 4.14: Splitting-tensile load-time curves for HSC and CFR-HSC having (a) 25 mm (b) 50 mm and (c) 75 mm long fibers

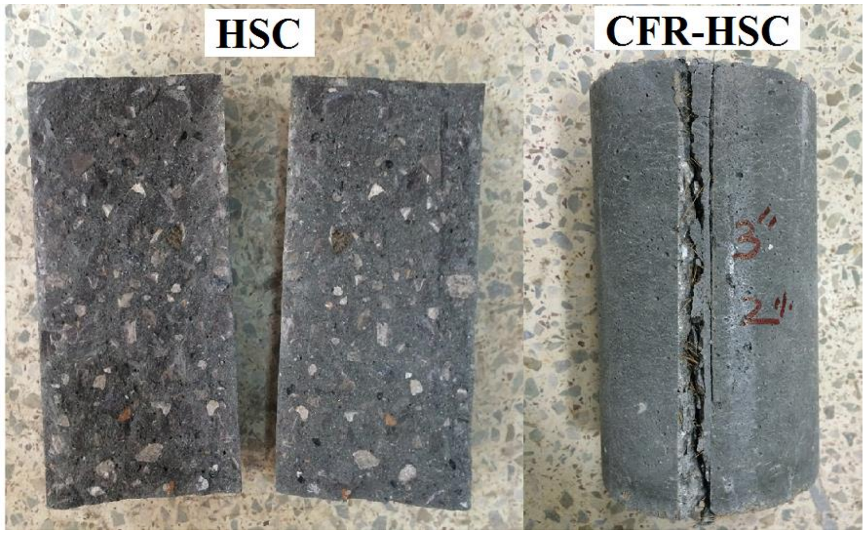

Figure 4.15: HSC and CFR-HSC specimens after STS test

4.4.2. Splitting-tensile strength (STS)

STS is calculated from the maximum load taken from splitting-tensile load-time curve. Figure 4.16 shows the effect on STS with increasing fiber length and content. The solid straight line shows the STS of HSC. With increase in fiber length CFR-HSC having 0.5% and 1% fiber content STS kept on increasing while with 1.5% and 2% fiber content STS first increases and then slightly reduces. STS decreases with increasing fiber content. However, in case of 50 mm fiber length STS has the maximum value at 1.5% fiber content which is 20.4% increased than that of HSC. For shorter fiber length STS of CFR-HSC was less than that of HSC because of insufficient embedment length for bridging the cracks. For longer fibers sufficient embedment length was available for bridging the cracks resulting in increased STS than that of HSC. At higher fiber content STS of CFR-HSC reduced because of voids creation in the matrix and improper compaction due to less workability.

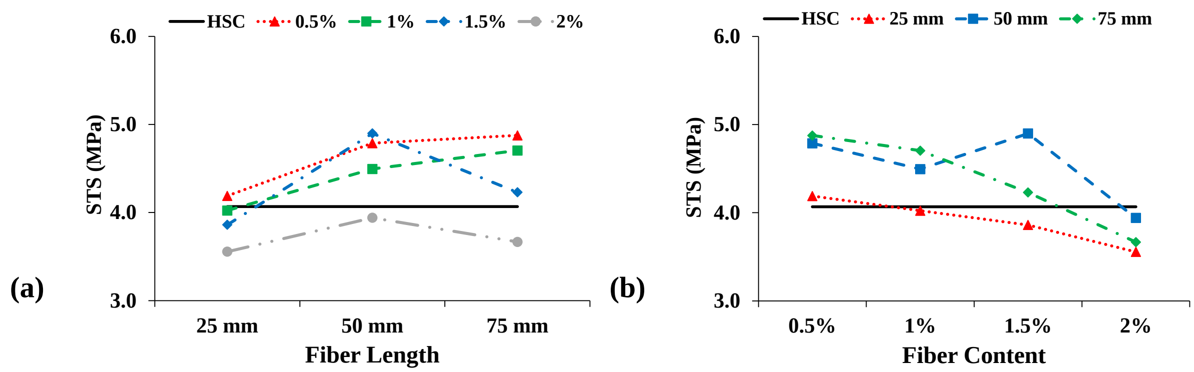

Figure 4.16: Influence on STS (a) fiber length (b) fiber content

4.4.3. Energy absorbed in splitting and toughness index

The area under the load-time curve up to the peak load is taken as pre-crack energy absorbed in splitting (PES). Cracked energy absorbed in splitting (CES) is taken as the area under the load-time curve from peak load to the ultimate load. Ultimate load is taken as the load at the point when test was stopped i.e. at 10 min. Total energy absorbed in splitting (TES) is calculated as the area under the load-time curve from zero to ultimate load. Toughness index in splitting (TIS) is the ratio of total energy absorbed in splitting to the pre-crack energy absorbed in splitting (i.e. TES/PES).

The influence on PES with increasing fiber length and content is shown in Figure 4.17. The solid straight line is PES of HSC. PES of CFR-HSC having 25 mm length is less than HSC. PES of CFR-HSC with 50 mm and 75 mm length has increased than HSC. The reason is 25 mm length fiber has shorter embedment length which results in pull-out of fibers at lower load value whereas 50 mm and 75 mm fibers has sufficient embedment length for bridging the cracks and provided significant resistant to load. PES of CFR-HSC decreases with increasing fiber content. The reason is the creation of air voids and improper compaction due to decreased workability with increasing fiber content. CFR-HSC with 50 mm fiber length and 1.5% content shows the maximum value which is increased by 36.7% than HSC. As far as fiber length is concerned, CFR-HSC having 0.5% and 1% fiber content, PES increases with increasing length. However, CFR-HSC having 1.5% and 2% fiber content, PES first increases and then decreases with increasing length. HSC sample suddenly broke in two pieces at peak load and there is no post-peak response of HSC. CFR-HSC samples were held together after the peak load and resists load up to some extent.

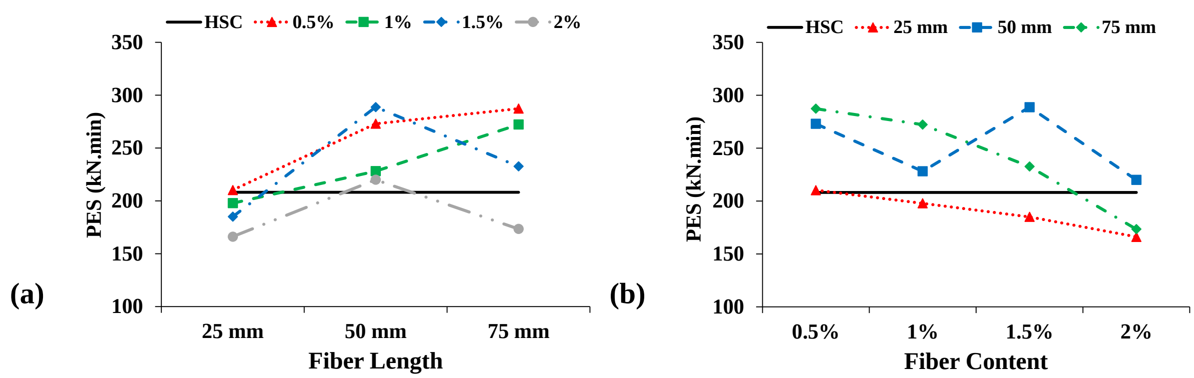

Figure 4.17: Influence on PES (a) fiber length (b) fiber content

The effect on CES with increasing fiber length and content is shown in Figure 4.18. CES increases with increasing fiber length and content. The possible reason is the bridging of cracks by fibers. However, in case of 1.5% and 2% fiber content, CES first increases and then decreases with increasing fiber length. The reasons may be the creation of air voids with higher fiber content and longer length and also improper compaction at the time of casting specimens due to less workability.

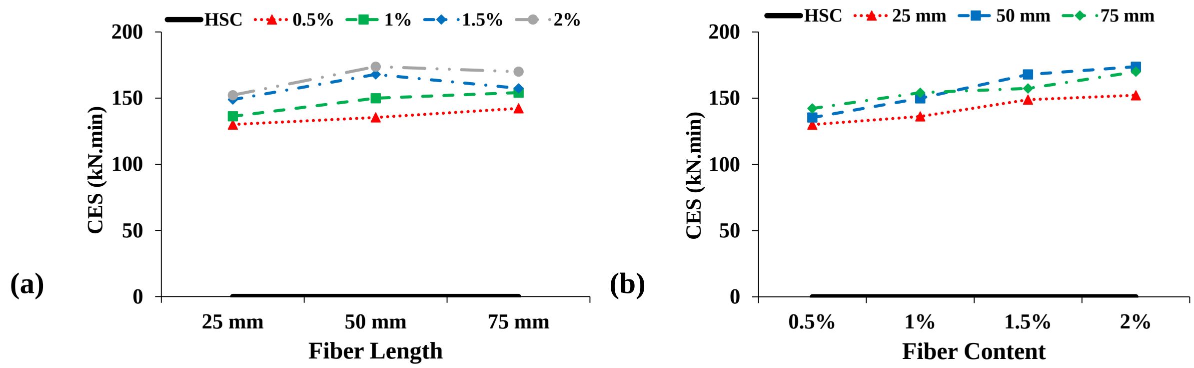

Figure 4.18: Influence on CES (a) fiber length (b) fiber content

The effect on TES with increasing fiber length and content is shown in Figure 4.19. Solid straight line is the TES of HSC. TES of CFR-HSC is always greater than HSC. TES of CFR-HSC decreases with increase in fiber length and content. However, TES of CFR-HSC having 1.5% and 2% fiber content first increases and then decreases with increasing fiber length.

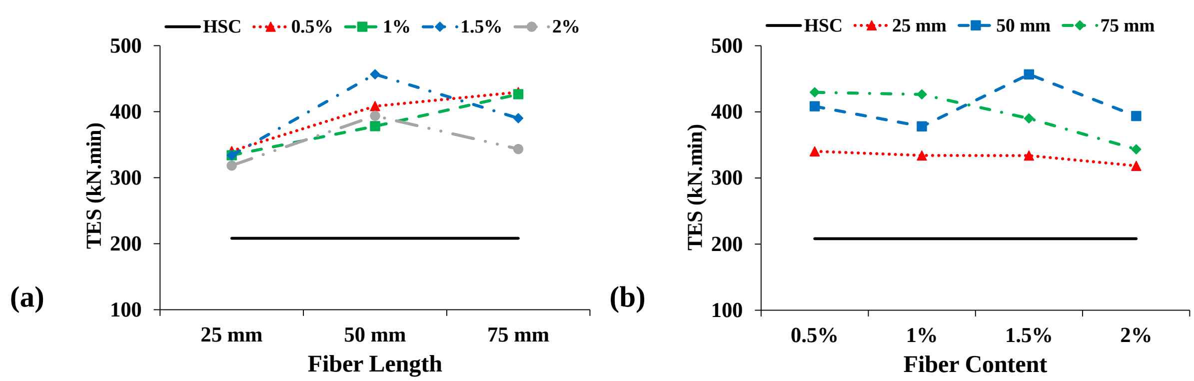

Figure 4.19: Influence on TES (a) fiber length (b) fiber content

The influence on TIS with increasing fiber length and content is shown in Figure 4.20. The solid straight is the TIS of HSC. TIS of CFR-HSC are increased than that of HSC. TIS decreases with increase in fiber length and increases with increasing fiber content.

However, CFR-HSC with 50 mm long fibers shows sudden drop in TIS at 1.5% content. This is due to its increased PES value. The TIS of CFR-HSC having 1.5% and 2% fiber content first decrease and then increases with increasing fiber length. All the splitting-tensile properties of HSC and CFR-HSC are shown in Table 4.5.

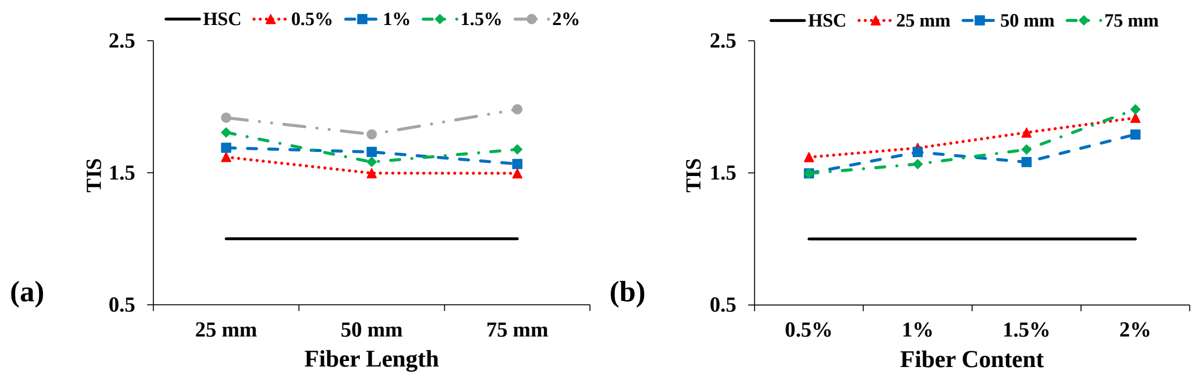

Figure 4.20: Influence on TIS (a) fiber length (b) fiber content

Table 4.5: Splitting-tensile properties of HSC and CFR-HSC

Mix ID	STS (MPa)	PES (kN.min)	CES (kN.min)	TES (kN.min)	TIS
Mix0	4.07	208.13	0.00	208.13	1.00
Mix1-0.5	4.19	210.20	130.00	340.20	1.62
Mix1-1	4.02	197.81	136.17	333.98	1.69
Mix1-1.5	3.86	185.00	148.82	333.82	1.80
Mix1-2	3.56	166.10	152.17	318.27	1.92
Mix2-0.5	4.79	272.95	135.37	408.32	1.50
Mix2-1	4.49	228.09	149.87	377.96	1.66
Mix2-1.5	4.90	288.71	167.87	456.58	1.58
Mix2-2	3.94	219.90	173.72	393.63	1.79
Mix3-0.5	4.88	287.23	142.22	429.45	1.50
Mix3-1	4.70	272.21	154.10	426.30	1.57
Mix3-1.5	4.23	232.61	157.31	389.92	1.68
Mix3-2	3.67	173.38	169.90	343.28	1.98

4.5. FLEXURAL PROPERTIES

4.5.1. Flexural behavior

During flexural-strength testing of beams, flexural load-displacement curves were recorded for all specimens. Flexural load-displacement curves for HSC and CFR-HSC are shown in Figure 4.21. HSC beams were broken into two pieces at peak load (Figure 4.22a). However, CFR-HSC were held together even after the peak load (Figure 4.22b). This is due to bridging effect of fibers in CFR-HSC beams which held the beam together after crack at peak load. To observe fiber failure mode in CFR-HSC, beams were intentionally broken into pieces. Coconut fiber failures observed were of two types, fiber pull-out and broken. Fiber pull-out decreased with increasing fiber length. The approximate percentage of fiber pull-out and broken with increasing fiber length is shown in Table 4.6 which is based on visual observations. The reason is for shorter fiber length, the embedment length of fiber in concrete is less resulting in increased pull-out failure. Whereas for longer fibers embedment length increases which resists the pull-out of fibers and results in increased broken failure.

Table 4.6: Approximate amount of fiber pull-out and broken with increasing length in flexural strength test

Fiber Length (mm)	Pull-out (%)	Broken (%)
25	25	75
50	15	85
75	10	90

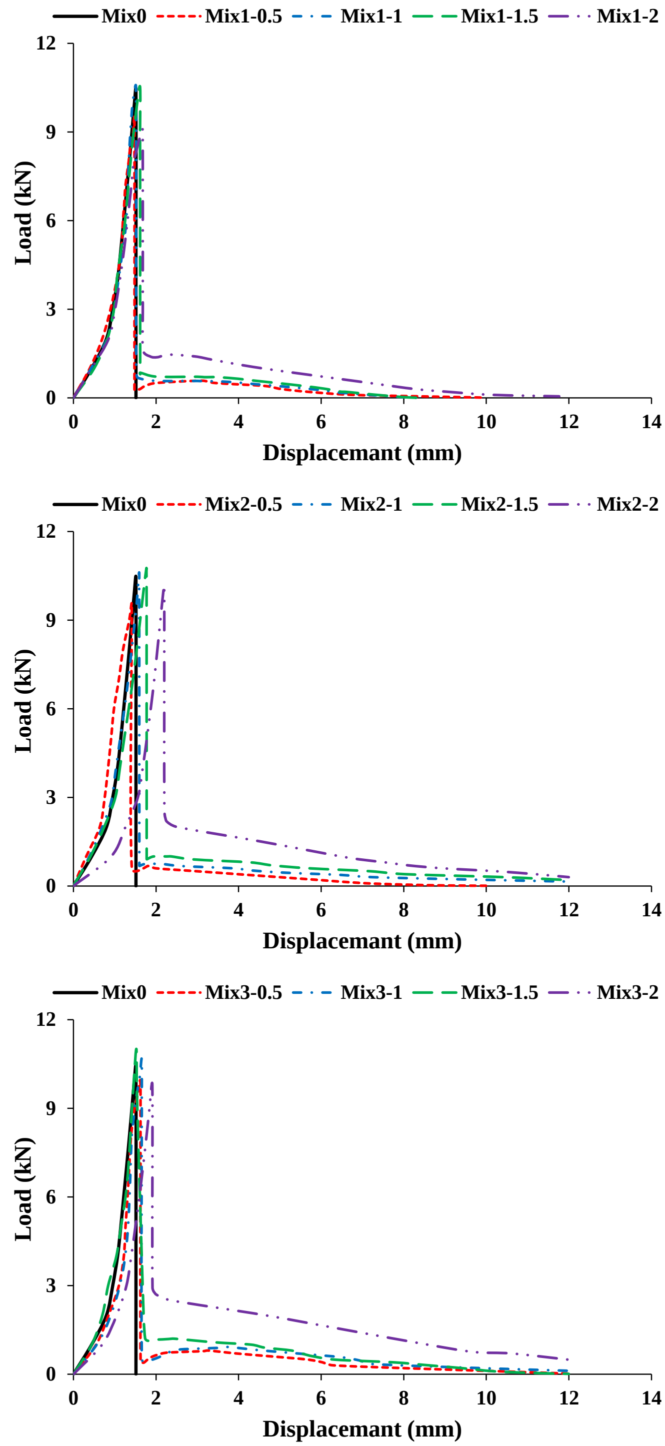

Figure 4.21: Load-displacement curves for HSC and CFR-HSC beams having (a) 25 mm (b) 50 mm and (c) 75 mm long fibers

(a) Tested HSC beam

(b) Tested CFR-HSC beam

(c) Fibers bridging in beam

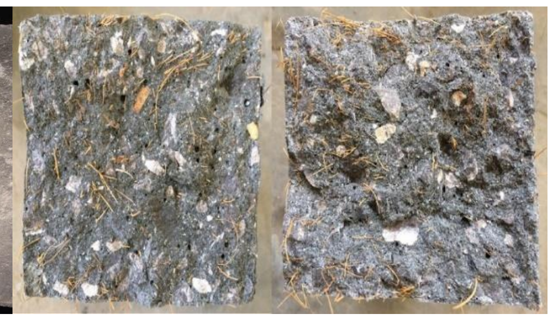

(d) Cross-section of tested CFR-HSC

Figure 4.22: Beams test

4.5.2. Modulus of rupture (MOR)

Modulus of rupture (MOR) is calculated from the peak load in load-displacement curve. Figure 4.23 shows the effect on MOR with increasing fiber length and content. The solid straight line indicates the MOR of HSC. MOR increases with increase in fiber length. Only with 2% fiber content MOR of CFR-HSC first increases and then decreases with increasing fiber length. With increase in fiber content up to 1.5%, MOR increases while decreases upon further increase in fiber content. Compared to HSC value MOR of CFR-HSC with 1.5% fiber content and 75 mm length increased by 5.4%. MOR of CFR-HSC with 0.5% fiber content is less than HSC. The reason is that at 0.5% fiber content, fibers are less in number and insufficient in resisting flexural load. MOR of CFR-HSC with

1% and 1.5% fiber content increased than HSC because there were sufficient amount of fibers to resist flexural load. With 2% fiber content of CFR-HSC, MOR is again less than that of HSC. The possible reasons may be: (i) higher fiber content results in dilution of cement; (ii) improper compaction at the time of casting specimens because of less workability; (iii) creation of air voids with higher fiber content.

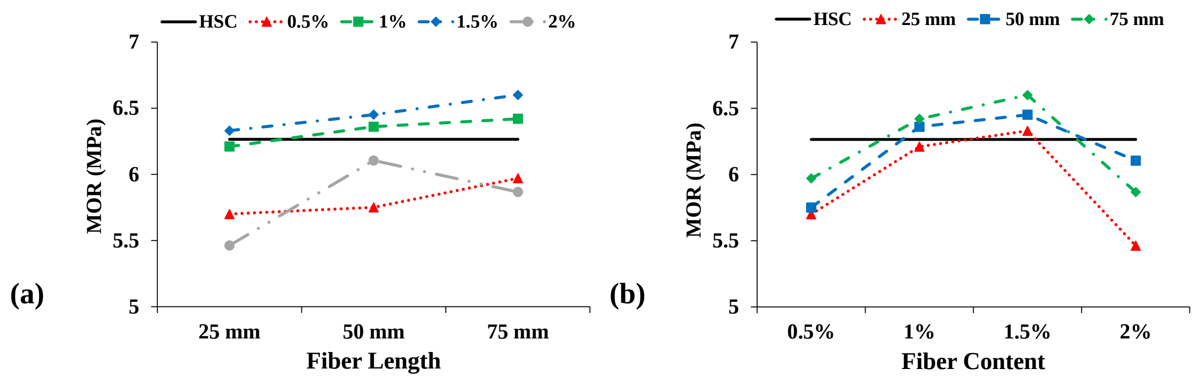

Figure 4.23: Influence on MOR (a) fiber length (b) fiber content:

4.5.3. Energy absorbed in flexure and toughness index

Pre-crack energy absorbed in flexure (PEF) is taken as the area under the load-displacement curve up to peak load. Cracked energy absorbed in flexure (CEF) is taken as the area under the load-displacement curve from peak load to the ultimate load. The ultimate load is taken as the load at which test is stopped. The total area under the load-displacement curve from zero to ultimate load is taken as the total energy absorbed in flexure (TEF). Toughness index in flexure (TIF) is the ratio of total energy absorbed in flexure to the pre-crack energy absorbed in flexure (i.e. TEF/PEF).

Figure 4.24 displays the influence on PEF with increasing fiber length and content. Solid straight line is the PEF of HSC. PEF of CFR-HSC is mostly higher than HSC. PEF first increases and then decreases with increasing fiber length. As longer fibers reduced the workability which results in decreased PEF. PEF increases with increasing fiber content up to 1.5% and then decreases on further increase in fiber content. The reasons may be improper compaction at the time of casting because of less workability and cement dilution with higher fiber content.

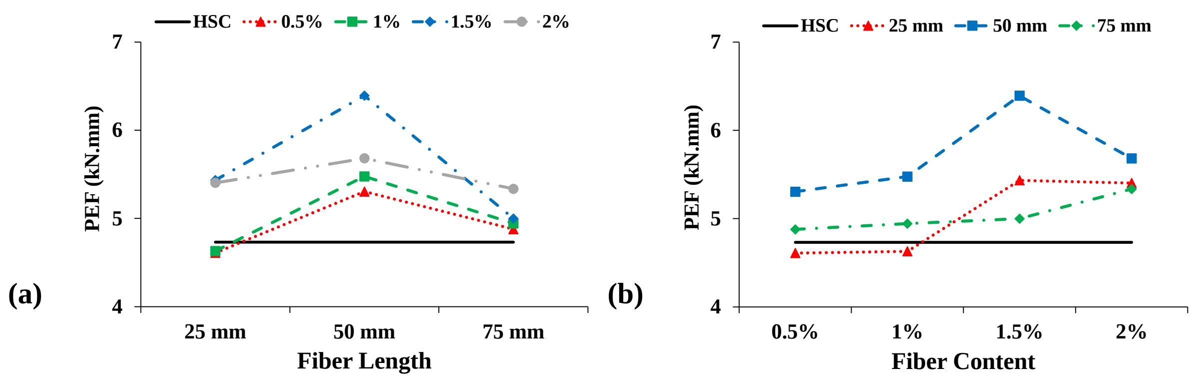

Figure 4.24: Influence on PEF (a) fiber length (b) fiber content

The effect on CEF with increasing fiber length and content is shown in Figure 4.25. CEF of HSC is zero as it was suddenly broken into two halves at peak load. With increasing fiber length CEF of CFR-HSC first increases and then decreases. The possible reasons are: (i) when fiber length is short embedment length of fibers in concrete is shorter that results in pull-out failure and lower CEF; (ii) with longer fibers embedment length of fibers in concrete increases and are able to resist significant flexure load before failure giving increased value of CEF; (iii) with increasing fiber content more fibers are available for bridging the cracks resulting in increased value of CEF. The CEF of CFR-HSC increases with increasing fiber content.

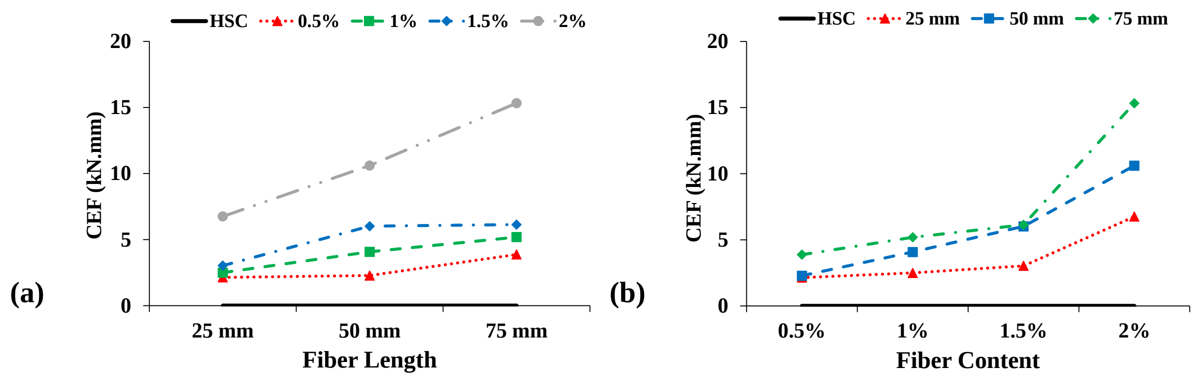

Figure 4.25: Influence on CEF (a) fiber length (b) fiber content

Figure 4.26 displays the influence on TEF with increasing fiber length and content. Solid straight line is TEF of HSC. TEF of HSC is less than CFR-HSC. TEF of CFR-HSC increases with increase in fiber length and content. TEF of CFR-HSC with 1.5% fiber content first increases and then slightly decreases with increasing length. CFR-HSC with 2% and 75 mm length has the maximum TEF value.

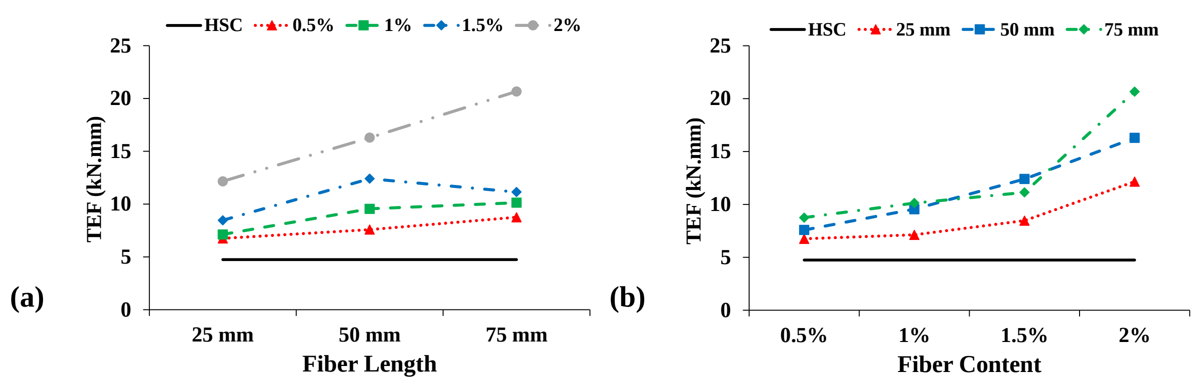

Figure 4.26: Influence on TEF (a) fiber length (b) fiber content

The influence on TIF with increasing fiber length and content is shown in Figure 4.27. Solid straight line is TIF of HSC. TIF of CFR-HSC is higher than HSC. TIF of CFR-HSC increases with increasing fiber length and content. The possible reasons are: (i) with increasing fiber content more fibers are available for bridging cracks which increases TEF and thus increasing TIF; (ii) with increasing fiber length embedment length of fibers increases and hence results in increased TIF. Table 4.7 shows all the flexural properties of HSC and CFR-HSC.

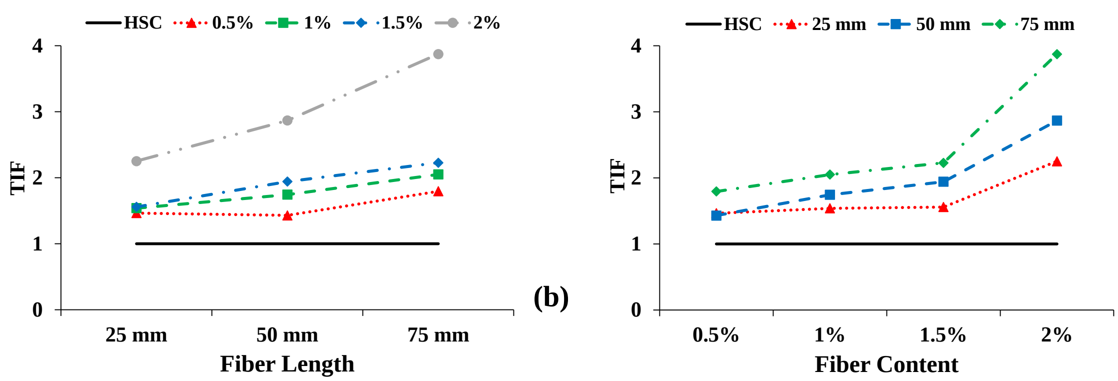

Figure 4.27: Influence on TIF (a) fiber length (b) fiber content

Table 4.7: Flexural properties of HSC and CFR-HSC

Mix ID	MOR (MPa)	PEF (kN.mm)	CEF (kN.mm)	TEF (kN.mm)	TIF
Mix0	6.26	4.73	0.00	4.73	1.00
Mix1-0.5	5.70	4.61	2.13	6.74	1.46
Mix1-1	6.21	4.63	2.49	7.12	1.54
Mix1-1.5	6.33	5.43	3.03	8.46	1.56
Mix1-2	5.46	5.40	6.75	12.15	2.25
Mix2-0.5	5.75	5.30	2.27	7.58	1.43
Mix2-1	6.36	5.48	4.07	9.55	1.74
Mix2-1.5	6.45	6.39	6.01	12.40	1.94
Mix2-2	6.10	5.68	10.60	16.28	2.87
Mix3-0.5	5.97	4.88	3.87	8.75	1.79
Mix3-1	6.42	4.94	5.18	10.13	2.05
Mix3-1.5	6.60	5.00	6.13	11.13	2.23
Mix3-2	5.87	5.34	15.32	20.66	3.87

4.6. MICROSTRUCTURE STUDY

SEM analysis was performed to study the microstructure of CFR-HSC. The samples for SEM analysis were prepared from CFR-HSC beams after performing flexural strength test. The objective of SEM analysis is to study the fiber-cement and aggregate-cement interfacial transition zones (ITZs), micro-cracks and voids in the matrix. The gap was observed at ITZ between fiber and cement paste (Figure 4.28 (a), (b)), which proves the fiber de-bonding failure. Form Figure 4.28 (c), and (f) it is observed that fiber addition in concrete create pores. Figure 4.28 (a), (b) and (e) shows the micro-cracks in the matrix. The approximate percentage of coconut fiber pull out and fiber broken in flexure is discussed earlier in section 4.5.1.

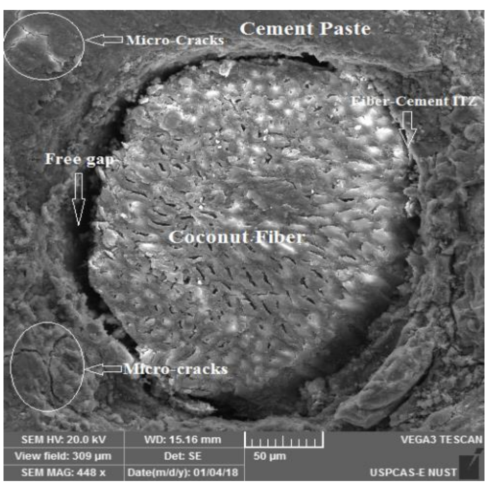

(a) Gap in fiber-cement ITZ and micro-cracks

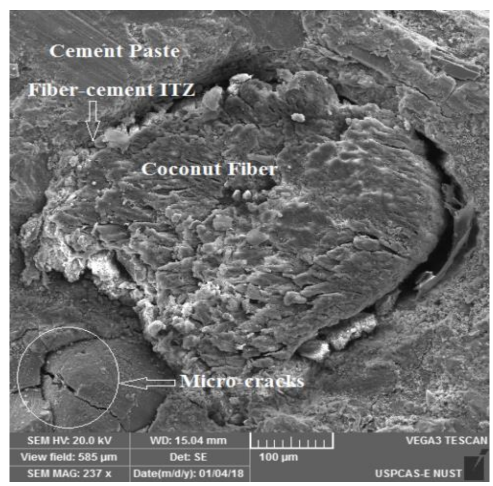

(b) Micro-cracks and fiber-cement ITZ

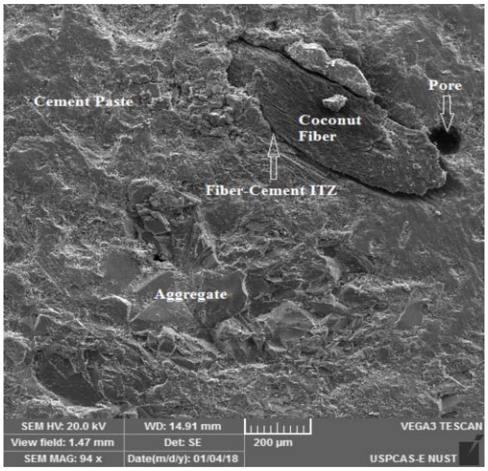

(c) Filled voids in the matrix

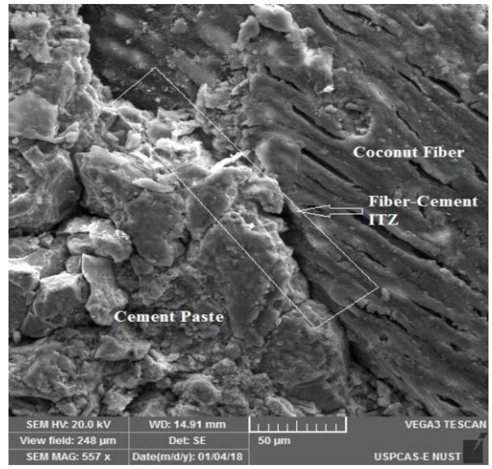

(d) Fiber-cement ITZ

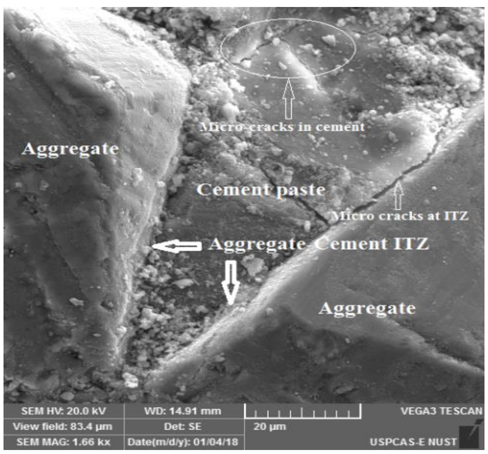

(e) Micro-cracks in cement paste and aggregate-cement ITZ

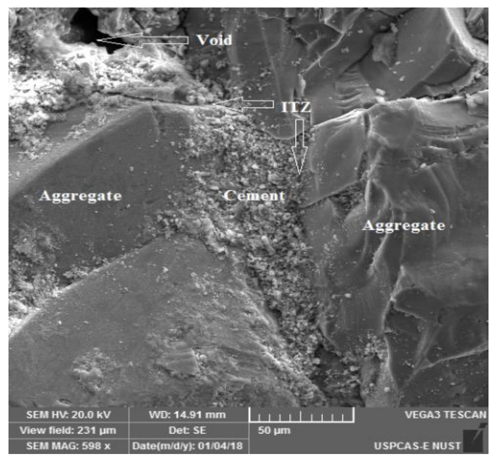

(f) Filled voids and aggregate-cement ITZ

Figure 4.28: Microstructure of CFR-HSC

CHAPTER 5

DISCUSSIONS

5.1. DISCUSSIONS AND OPTIMIZATION OF CF IN HSC

In this study, coconut fibers having lengths 25 mm, 50 mm and 75 mm and 0.5%, 1%, 1.5% and 2% content by mass of cement are incorporated in high strength concrete (HSC) having mix design ratio of 1:1.5:1.5 for cement, sand and aggregate. The water cement (W/C) ratio is kept at 0.35 for both HSC and CFR-HSC. Silica fume with 10% content as replacement of cement is added to improve the mechanical properties and super-plasticizer of 1% content, by mass of cement is added increase the workability of mix. Addition of coconut fibers in HSC not only increased σ, E_{static}, STS, MOR but it also improved post-cracking behavior in compression, splitting-tensile and flexure. Table 5.1 summarizes all the mechanical properties of HSC and CFR-HSC. Overall best properties are obtained from CFR-HSC with 50 mm long fibers and 1.5% fiber content, by mass of cement. The σ, TEC, μ, STS, TES, MOR and TEF of CFR-HSC with 50 mm long fibers and 1.5% content are increased by 24.8%, 71.2%, 14.4%, 20.4%, 120%, 3% and 162%, respectively, than that of HSC. Whereas, for the same CFR-HSC slump and E_{static} reduced by 50% and 8%, respectively, than that of HSC.

ACI committee 234 reported that use of silica fume as replacement of cement in concrete decreases permeability, increases durability and resistant to chemical attack. Thus concrete having silica fume would ensure better performance in hydraulic and under-water structures. Also in addition to silica fume incorporation of coconut fibers in concrete would have better durability properties and resistance to deleterious effects in aggressive environment (i.e. under-water structures) as also reported by Ramli et al. (2013).

Table 5.1: Mechanical properties consequence of HSC and CFR-HSC

Concrete Type	E_{static} (GPa)	σ (MPa)	TEC (MPa)	μ	STS (MPa)	TES (kN.min)	MOR (MPa)	TEF (kN.mm)	Density (kg/m^3)
HSC	50.21	49.14	0.052	1.11	4.07	208	6.26	4.73	2328
CFR-HSC with maximum values	52.14 (0.5%, 25 mm)	66.9 (0.5%, 50 mm)	0.089 (1.5%, 50 mm)	1.27 (1.5%, 50 mm)	4.90 (1.5%, 50 mm)	457 (1.5%, 50 mm)	6.60 (1.5%, 75 mm)	20.66 (2%, 75 mm)	2326 (0.5%, 50 mm)
CFR-HSC with minimum values	43.46 (2%, 75 mm)	41.36 (2%, 50 mm)	0.050 (2%, 75 mm)	1.14 (0.5%, 25 mm)	3.56 (2%, 25 mm)	318 (2%, 25 mm)	5.46 (2%, 25 mm)	6.74 (0.5%, 50 mm)	2266 (2%, 75 mm)
Recommended CFR-HSC (1.5% fiber content, 50 mm long fibers)	45.85	61.34	0.089	1.27	4.90	457	6.45	12.4	2310

Splitting-tensile and flexure behavior of HSC and CFR-HSC reveals that incorporation of fibers in HSC controlled the brittleness of HSC by bridging the cracks, thus improving ductility property. The improved strain ductility and better post-cracking behavior favoring the utility of CFR-HSC for civil engineering applications like high rise buildings, long span bridges and hydraulic structures.

5.2. COMPARISON OF CFR-HSC COMPRESSIVE PROPERTIES W.R.T HSC

The comparison of compressive properties of HSC and CFR-HSC are shown in Figure 5.1. With optimized CFR-HSC (Mix2-1.5) the σ, PEC, CEC, PCEC, TEC, TIC and μ increased by 24.8%, 40%, 186%, 325%, 73.1%, 23.6% and 14.6%, respectively, as compared to that of HSC. However, with the same CFR-HSC E_{static} decreased by 8.7%

than that of HSC. The possible reasons for the improved properties of CFR-HSC than that of HSC are;

(i) Fibers restrained crack extension and delayed cracks growth rate which results in increased σ of CFR-HSC.

(ii) Incorporation of CF results in elastic behavior thus reducing E_{static}.

(iii) The improved energy absorption of CFR-HSC is due to fiber bridging effect and better post-cracking behavior.

(iv) Fiber bridging the cracks results in higher strain values after the yield stress and hence higher μ is achieved.

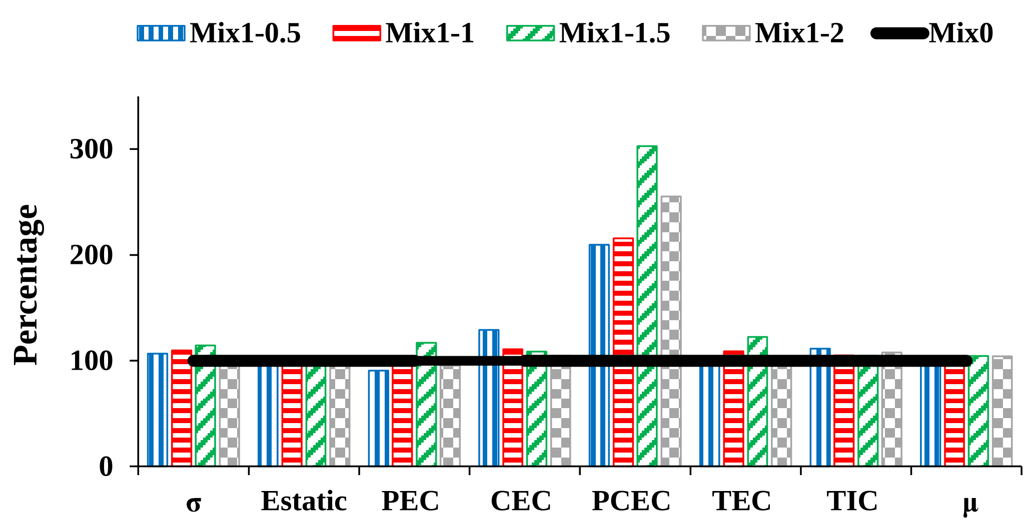

(a)

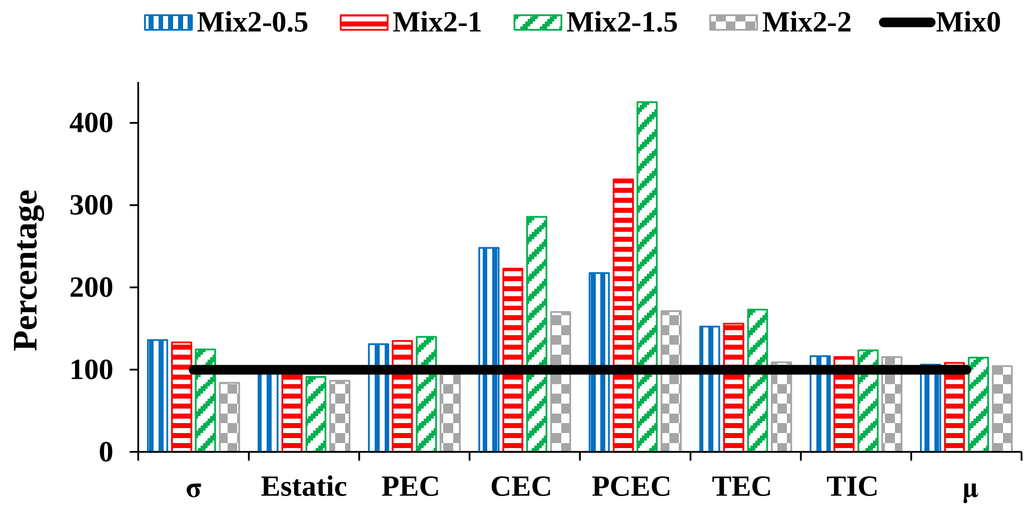

(b)

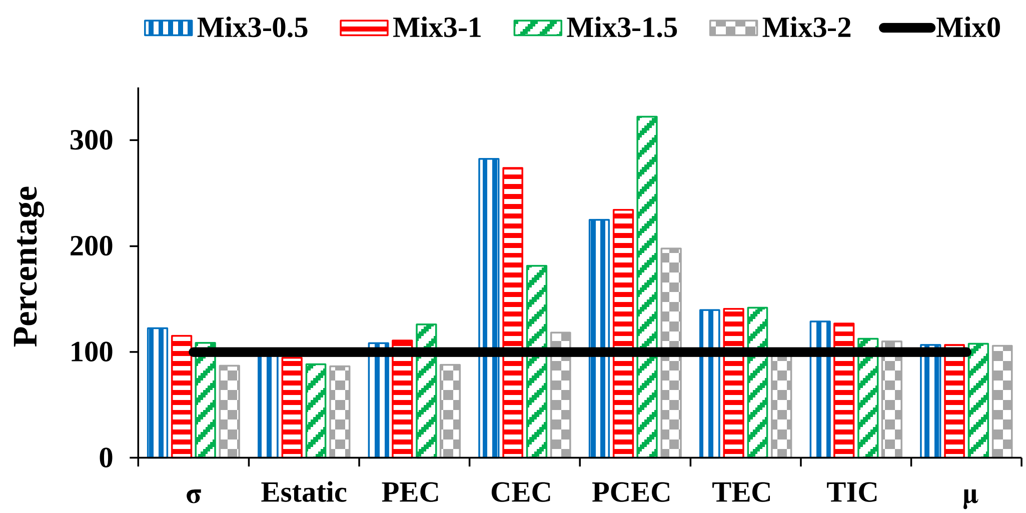

(c)

Figure 5.1: Comparison of compressive properties of HSC and CFR-HSC with (a) 25 mm, (b) 50 mm and (c) 75 mm long fibers

5.3. COMPARISON OF CFR-HSC SPLITTING-TENSILE PROPERTIES W.R.T HSC

The comparison of splitting-tensile properties of HSC and CFR-HSC are shown in Figure 5.2. With optimized CFR-HSC (Mix2-1.5) the STS, PES, TES and TIS increased by 20.4%, 38.7%, 119% and 58.1%, respectively, as compared to that of HSC. As HSC sample suddenly broken in to two halves at peak load, thus giving no CES value while all CFR-HSC have significant CES values results in increased TES. The reasons for improved splitting-tensile properties of CFR-HSC are improved microstructure and fiber bridging effect.

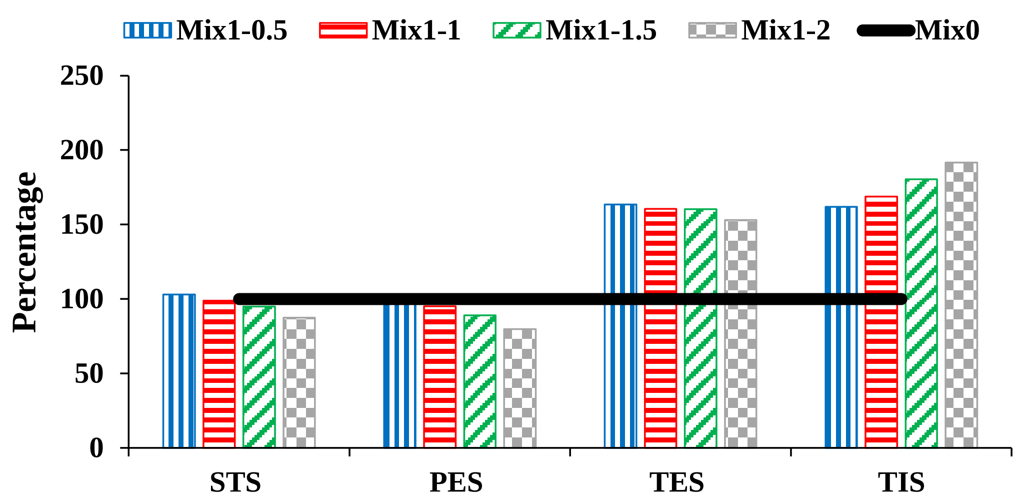

(a)

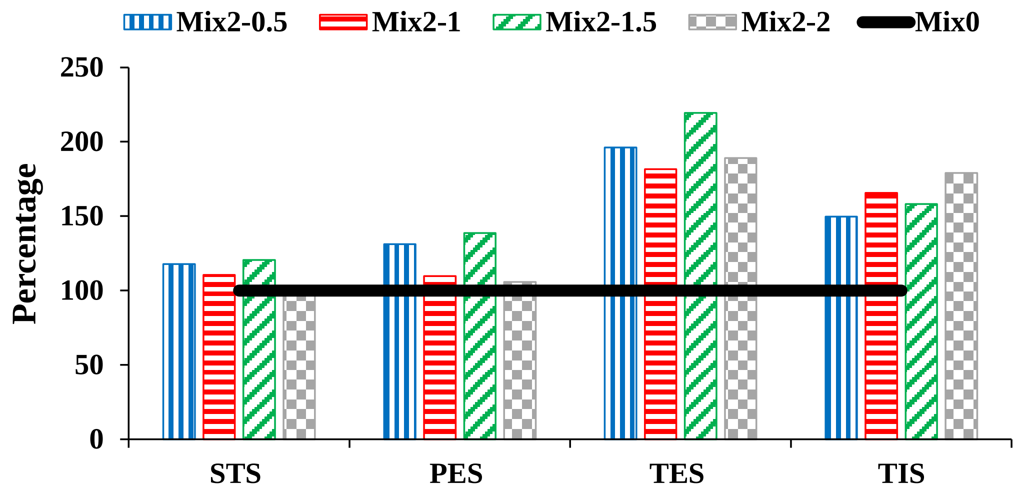

(b)

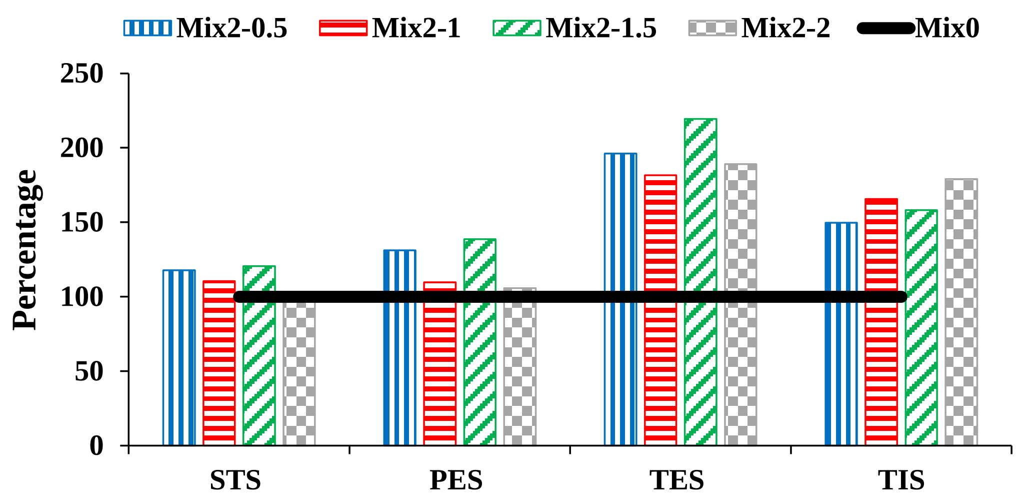

(c)

Figure 5.2: Comparison of splitting-tensile properties of HSC and CFR-HSC with (a) 25 mm, (b) 50 mm and (c) 75 mm long fibers

5.4. COMPARISON OF HSC AND CFR-HSC FLEXURAL PROPERTIES

The comparison of flexural properties of HSC and CFR-HSC are shown in Figure 5.3. With optimized CFR-HSC the MOR, PEF, TEF and TIF increased by 3%, 35.1%, 162% and 94%, respectively, as compared to that of HSC. HSC beam suddenly broken in to two halves at peak load during flexural strength test, thus giving no CEF value while all CFR-HSC showed significant CEF values results in increased TEF. The reasons are already explained in section 4.5.3.

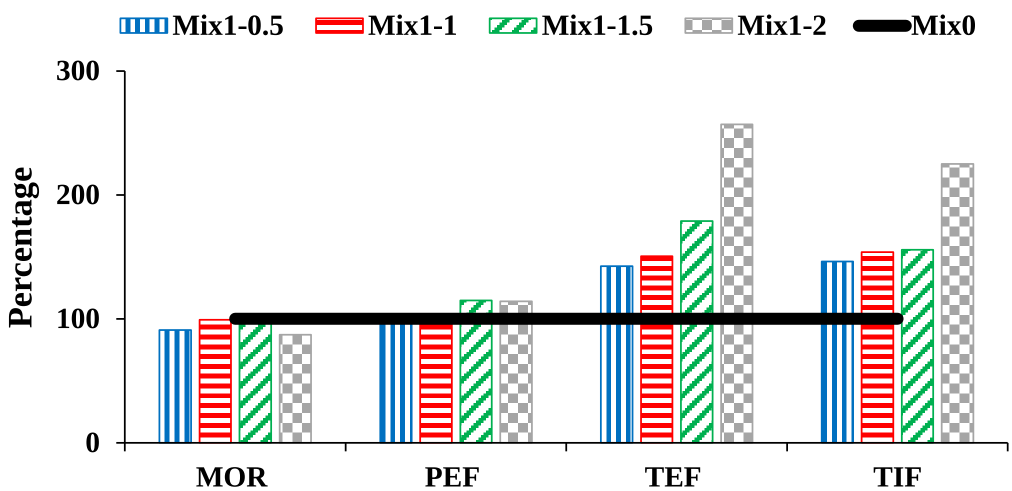

(a)

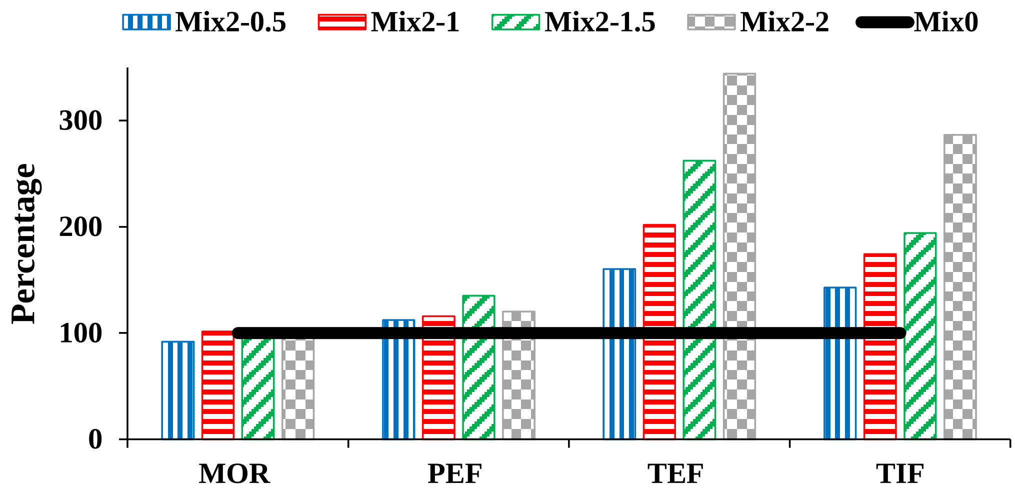

(b)

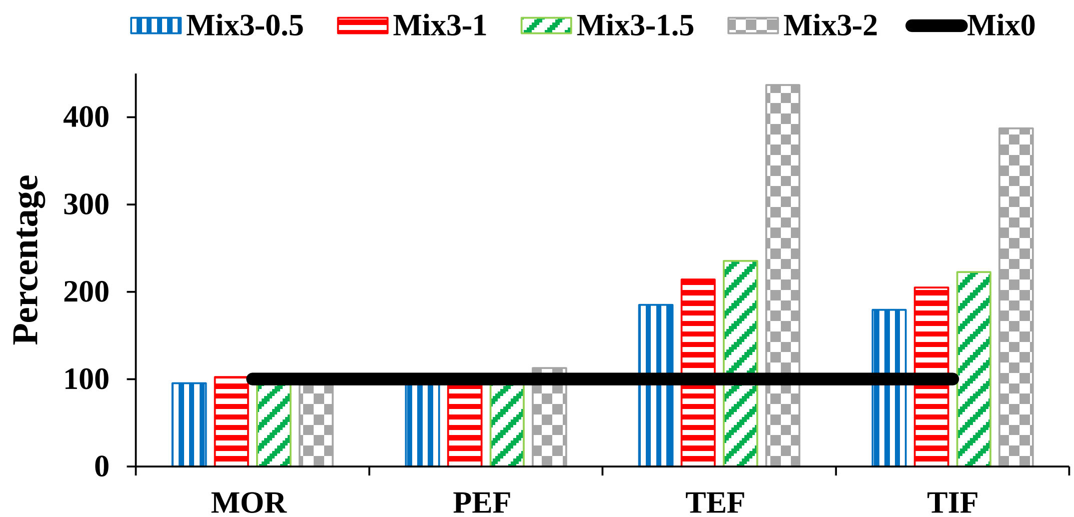

(c)

Figure 5.3: Comparison of flexural properties of HSC and CFR-HSC with (a) 25 mm, (b) 50 mm and (c) 75 mm long fibers

CHAPTER 6

CONCLUSIONS AND RECOMMENDATIONS

6.1. CONCLUSIONS

In this study, coconut fibers of different lengths (25 mm, 50 mm and 75 mm) and different contents (0.5%, 1%, 1.5% and 2%, by mass of cement) are added in high strength concrete (HSC) to investigate its mechanical properties for civil engineering applications. The results of coconut fiber reinforced high strength concrete (CFR-HSC) are compared with that of HSC having same mix design. The following conclusions are made based on the experimental work:

- Slump and density of CFR-HSC is decreased as compared to that of HSC. With changing fiber length and content, slump of CFR-HSC decreased from 7.5% - 87.5% and density up to 2.7% than HSC.
- The compressive strength (σ) of CFR-HSC is increased with lower fiber content while decreased with higher fiber content than that of HSC. The σ of CFR-HSC with 50 mm long fibers and 1.5% fiber content increased by 25% than that of HSC.
- There is an increase of 20.4% and 3% in splitting-tensile and flexural strengths, respectively, for CFR-HSC having 50 mm long fibers and 1.5% content, when compared to that of HSC.
- In comparison to HSC, the total energy absorbed in compression, splitting and flexure of CFR-HSC with 50 mm long fibers and 1.5% fiber content are

increased by 72.5%, 119% and 162%, respectively. Also toughness index in compression, splitting and flexure for the same CFR-HSC is increased by 23.4%, 58% and 94%, respectively, than that of HSC.

- CFR-HSC with 50 mm long fibers and 1.5% fiber content show the maximum strain ductility which is 14.6% increased than HSC.
- From splitting-tensile and flexure behaviors of HSC and CFR-HSC, it is concluded that incorporation of coconut fibers controlled the brittleness by enhancing the ductility of HSC up to some extent.
- The best overall results for CFR-HSC are observed with addition of 50 mm long coconut fibers and 1.5% fiber content.

Based on above results, the improved mechanical properties of CFR-HSC with 50 mm long coconut fibers and 1.5% fiber content favoring its utility for civil engineering applications like high rise buildings, long span bridges and hydraulic structures.

6.2. RECOMMENDATIONS

- Experimental study of CFR-HSC in structural members needs to be carried out.
- Long-term durability of CFR-HSC needs to be investigated before practical implementation.
- Dynamic properties of CFR-HSC needs to be investigated to study the influence of coconut fibers in HSC under dynamic loadings.
- Analytical model of CFR-HSC needs to be developed.

REFERENCES

Afroughsabet, V., & Ozbakkaloglu, T. (2015). Mechanical and durability properties of high-strength concrete containing steel and polypropylene fibers. *Construction and building materials*, *94*, 73-82.

Aggarwal, L. K. (1992). Studies on cement-bonded coir fibre boards. *Cement and Concrete Composites*, *14*(1), 63-69.

Al-Oraimi, S. K., & Seibi, A. C. (1995). Mechanical characterisation and impact behaviour of concrete reinforced with natural fibres. *Composite Structures*, *32*(1-4), 165-171.

Ali, M., Li, X., & Chouw, N. (2013). Experimental investigations on bond strength between coconut fibre and concrete. *Materials & Design*, *44*, 596-605.

Ali, M., Liu, A., Sou, H., & Chouw, N. (2012). Mechanical and dynamic properties of coconut fibre reinforced concrete. *Construction and Building Materials*, *30*, 814-825.

Aldred, J. M., Holland, T. C., Morgan, D. R., Roy, D. M., Bury, M. A., Hooton, R. D...... & Ozyildirim, H. C. (2006). Guide for the use of silica fume in concrete. Reported by ACI–American Concrete Institute–Committee, 234.

ASTM C143/C143M-15a, Standard Test Method for Slump of Hydraulic-Cement Concrete, *https://www.astm.org.*

ASTM C138 / C138M - 17a, Standard Test Method for Density (Unit Weight), Yield, and Air Content (Gravimetric) of concrete, *https://www.astm.org.*

ASTM C39/C39M-17b, Standard Test Method for Compressive Strength of Cylindrical Concrete Specimens, *https://www.astm.org.*

ASTM C496/C496M-17, Standard Test Method for Splitting Tensile Strength of Cylindrical Concrete Specimens, *https://www.astm.org.*

ASTM C293/C293M-16, Standard Test Method for Flexural Strength of Concrete (Using Simple Beam with Center-Point Loading, *https://www.astm.org.*

Aziz, M. A., Paramasivam, P., & Lee, S. L. (1981). Prospects for natural fibre reinforced concretes in construction. International Journal of Cement Composites and Lightweight Concrete, 3(2), 123-132.

Breitenbuecher, R. (1999). High-performance fiber concrete SIFCON for repairing environmental structures. In *Proceedings of the third RILEM/ACI workshop: high-performance fiber reinforced cement composites, London, UK* (pp. 585-94).

Brandt, A. M. (2008). Fibre reinforced cement-based (FRC) composites after over 40 years of development in building and civil engineering. *Composite structures*, *86*(1), 3-9.

Baruah, P., & Talukdar, S. (2007). A comparative study of compressive, flexural, tensile and shear strength of concrete with fibres of different origins. *Indian concrete journal*, *81*(7), 17-24.

Chan, S. Y. N., Feng, N. Q., & Tsang, M. K. C. (2000). Durability of high-strength concrete incorporating carrier fluidifying agent. *Magazine of Concrete Research*, *52*(4), 235-242.

Eren, Ö., & Celik, T. (1997). Effect of silica fume and steel fibers on some properties of high-strength concrete. Construction and Building Materials, 11(7-8), 373-382.

Eswari, S., Raghunath, P. N., & Suguna, K. (2008). Ductility performance of hybrid fibre reinforced concrete. *American Journal of Applied Sciences*, *5*(9), 1257-1262.

Ezeldin, A., & Balaguru, P. (1989). Bond behavior of normal and high-strength fiber reinforced concrete. *Materials Journal*, *86*(5), 515-524.

Farnam, Y., Mohammadi, S., & Shekarchi, M. (2010). Experimental and numerical investigations of low velocity impact behavior of high-performance fiber-reinforced cement based composite. *International Journal of Impact Engineering*, *37*(2), 220-229.

French et al. (1998). High-strength concrete applications to pre-stressed bridge girders.

Hassan, K. E., Cabrera, J. G., & Maliehe, R. S. (2000). The effect of mineral admixtures on the properties of high-performance concrete. Cement and concrete composites, 22(4), 267-271.

http://www.naturalfibres2009.org/en/fibres/coir.html

Khan, M., & Ali, M. (2018). Effectiveness of hair and wave polypropylene fibers for concrete roads. Construction and Building Materials, 166, 581-591.

Khan, M., & Ali, M. (2016). Use of glass and nylon fibers in concrete for controlling early age micro cracking in bridge decks. *Construction and Building Materials*, *125*, 800-808.

John, V. M., Cincotto, M. A., Sjöström, C., Agopyan, V., & Oliveira, C. T. A. (2005). Durability of slag mortar reinforced with coconut fibre. Cement and Concrete Composites, 27(5), 565-574.

Johari, M. M., Brooks, J. J., Kabir, S., & Rivard, P. (2011). Influence of supplementary cementitious materials on engineering properties of high strength concrete. Construction and Building Materials, 25(5), 2639-2648.

Kuder, K. G., & Shah, S. P. (2010). Processing of high-performance fiber-reinforced cement-based composites. *Construction and Building Materials*, *24*(2), 181-186.

Li, Z., Wang, L., & Wang, X. (2006). Flexural characteristics of coir fiber reinforced cementitious composites. Fibers and Polymers, 7(3), 286-294.

Lim, J. C., & Ozbakkaloglu, T. (2014). Influence of silica fume on stress–strain behavior of FRP-confined HSC. *Construction and Building Materials*, *63*, 11-24.

Mazloom, M., Ramezanianpour, A. A., & Brooks, J. J. (2004). Effect of silica fume on mechanical properties of high-strength concrete. Cement and Concrete Composites, 26(4), 347-357.

Mbessa, M., & Péra, J. (2001). Durability of high-strength concrete in ammonium sulfate solution. *Cement and concrete research*, *31*(8), 1227-1231.

Munawar, S. S., Umemura, K., & Kawai, S. (2007). Characterization of the morphological, physical, and mechanical properties of seven nonwood plant fiber bundles. *Journal of Wood Science*, *53*(2), 108-113.

Nili, M., & Afroughsabet, V. (2010). Combined effect of silica fume and steel fibers on the impact resistance and mechanical properties of concrete. *International Journal of Impact Engineering*, *37*(8), 879-886.

Peterman, Mark B., and Ramon L. Carrasquillo. "Production of high strength concrete." (1986).

Rabbat, B. G., & Russell, H. G. (1982). *Optimized sections for precast, prestressed bridge girders* (No. RD080. 01E). Portland Cement Association, Research and Development/Construction Technology Laboratories.

Rashiddadash, P., Ramezanianpour, A. A., & Mahdikhani, M. (2014). Experimental investigation on flexural toughness of hybrid fiber reinforced concrete (HFRC) containing metakaolin and pumice. *Construction and Building Materials*, *51*, 313-320.

Ramli, M., Kwan, W. H., & Abas, N. F. (2013). Strength and durability of coconut-fiber-reinforced concrete in aggressive environments. *Construction and Building Materials*, *38*, 554-566.

Reis, J. M. L. (2006). Fracture and flexural characterization of natural fiber-reinforced polymer concrete. Construction and building materials, 20(9), 673-678.

Slate, F. O. (1976). Coconut fibres in concrete. Engineering Journal of Singapore, 3(1), 51-54.

Song, P. S., & Hwang, S. (2004). Mechanical properties of high-strength steel fiber-reinforced concrete. Construction and Building Materials, 18(9), 669-673.

State-of-the-Art Report on High-Strength Concrete, ACI 363R-92, ACI Committee 363 Report, American Concrete Institute, Detroit, 1992.

Swamy, R. N. (1985). High-strength concrete-material properties and structural behavior. *Special Publication*, *87*, 119-146.

Yazici, H. (2007). The effect of curing conditions on compressive strength of ultra-high strength concrete with high volume mineral admixtures. *Building and environment*, *42*(5), 2083-2089.

Zia, A., & Ali, M. (2017). Behavior of fiber reinforced concrete for controlling the rate of cracking in canal-lining. Construction and Building Materials, 155, 726-739.